

Portland State University

PDXScholar

Civil and Environmental Engineering Faculty
Publications and Presentations

Civil and Environmental Engineering

11-1-2022

Cyclic Porewater Pressure Generation in Intact Silty Soils

Arash Khosravifar

Portland State University, karash@pdx.edu

Stephen Dickenson

Diane Moug

Portland State University, dmoug@pdx.edu

Follow this and additional works at: https://pdxscholar.library.pdx.edu/cengin_fac



Part of the [Civil and Environmental Engineering Commons](#)

Let us know how access to this document benefits you.

Citation Details

Published as: Khosravifar, A., Dickenson, S., & Moug, D. (2022). Cyclic porewater pressure generation in intact silty soils. *Soil Dynamics and Earthquake Engineering*, 162, 107482.

This Pre-Print is brought to you for free and open access. It has been accepted for inclusion in Civil and Environmental Engineering Faculty Publications and Presentations by an authorized administrator of PDXScholar. Please contact us if we can make this document more accessible: pdxscholar@pdx.edu.

Cyclic Porewater Pressure Generation in Intact Silty Soils

Arash Khosravifar^{1,*}, Stephen Dickenson², Diane Moug³

¹ Assistant Professor, Department of Civil and Environmental Engineering, Portland State University, Portland, OR 97201; e-mail: karash@pdx.edu

² Principal Engineer, New Albion Geotechnical, Inc., Reno, NV 89509; e-mail: sed@newalbiongeotechnical.com

³ Assistant Professor, Department of Civil and Environmental Engineering, Portland State University, Portland, OR 97201; e-mail: dmoug@pdx.edu

ABSTRACT

The results of cyclic strain-controlled, constant volume direct simple shear (CDSS) tests and field shaking tests have been evaluated for intact, natural, low-plastic silts from six different fine-grained soils with 54% to 100% fines content, 47% to 83% silt content, and plasticity indices (PI) ranging from nonplastic to 16. These tests constitute a subset of a larger archive of CDSS tests performed on silt deposits from the Pacific Northwest, British Columbia, and Alaska collected and analyzed by the co-authors. The cyclic data are presented in this paper for two objectives: (a) to characterize cyclically-induced excess pore pressure generation in intermediate soils with various soil index properties and stress histories, and (b) to provide calibrated Vucetic and Dobry model parameters for simulating excess pore pressure generation in the silt soils based on the data and trends presented in the first objective. The CDSS test results showed that excess pore pressure ratios decrease with PI over the narrow range of PI evaluated and decrease with overconsolidation ratio. The cyclic threshold shear strain amplitude for pore pressure generation extracted from field shaking tests on silts were within the range proposed in the literature, confirming that the cyclic threshold shear strain amplitude is a fundamental soil property. Calibrated Vucetic and Dobry model parameters for these intermediate, fine-grained silts were

* Corresponding author.

E-mail address: karash@pdx.edu (A. Khosravifar)

27 significantly different than those reported for sands in the literature and were heavily influenced
28 by the overconsolidation ratio. The calibrated parameters obtained in this study can be used as a
29 benchmark in selecting model parameters for silts.

30 **Keywords:** Cyclic behavior of silts, cyclic pore water pressure, strain-controlled CDSS,
31 intermediate soils

32

33 1 INTRODUCTION

34 Silt-rich soil deposits are prevalent in the Pacific Northwest region of the USA as well as other
35 parts of the world. While the majority of past research has been focused on the cyclic behavior of
36 sands and clays, few studies have investigated the cyclic response of intermediate fine-grained
37 soils that fall in between classical sand and clay types. The cyclic behavior of silt has been
38 documented as intermediate between the generalized and short-hand characterization of soil
39 behavior as either “sand-like” or “clay-like”, thereby adding a level of complexity to seismic
40 vulnerability studies involving silt.

41 Several studies have investigated the effects of fines content (FC) on cyclic strength of silty sands,
42 and the conclusions of these studies vary. While some studies report that the cyclic strength of
43 soils decreases with increasing FC (e.g. Shen et al. 1977, Troncoso and Verdugo 1985, Vaid
44 1994), other studies report that cyclic resistance decreases up to a limiting silt content beyond
45 which the cyclic strength increases with FC (e.g. Koester 1994, Polito and Martin 2001). Polito
46 and Martin (2001) found that this limiting silt content—where the soil behavior transitions from
47 being governed by its coarse fraction to being governed by its fine fraction—ranges between 25%
48 to 40% for most soils. Hazirbaba and Rathje (2009) reported that the excess pore pressure of
49 sand decreases (i.e., equivalent to an increase in cyclic resistance) up to a FC of 10%; beyond
50 that point, it either levels off or increases for FC up to 20%. A similar trend was reported by
51 Mousavi and Ghayoomi (2020). The abovementioned studies focus on sands with non-plastic
52 fines, and most were based on testing programs using reconstituted samples.

53 While tests on reconstituted samples aid in understanding the fundamental soil behavior on close-
54 to-identical specimens, the implications of the findings for naturally deposited soils need to be
55 investigated. This is particularly important, as naturally deposited soils with higher FC also tend
56 to have a higher PI (Mitchell and Soga 2005). As shown by the results of many studies, the cyclic
57 resistance of soils tends to increase with PI (e.g., Bray and Sancio 2006, Idriss and Boulanger
58 2006). A number of studies have investigated the cyclic resistance of silts with respect to PI using
59 stress-controlled cyclic shear tests on intact specimens (e.g., Dahl et al. 2014, 2018;
60 Wijewickreme et al. 2019). While stress-controlled tests are useful in characterizing the cyclic
61 shear resistance for “triggering liquefaction”, defined as pore pressure ratios of ~100% or some
62 level of large shear strain (e.g., 3.0 to 3.75%), strain-controlled tests are often used to characterize
63 the development of excess pore pressure with loading cycles over a range of shear strain
64 amplitudes. In a few studies, strain-controlled tests were conducted to characterize the pore
65 pressure generation of intact plastic silt specimens with PIs ranging from 17 to 39 (Jana and
66 Stuedlein 2021); however, very little published data can be found on pore pressure generation of
67 low plasticity silts in strain-controlled cyclic shear tests. The study presented here attempts to fill
68 this gap by reporting on strain-controlled cyclic shear tests performed on natural, intact, low-
69 plasticity silts with PIs ranging from nonplastic (NP) to 16. The results of the study have practical
70 implications, considering that the cyclic behavior of fine-grained soils that fall in this range of PI
71 may be characterized differently based on commonly used screening methods (e.g., Bray and
72 Sancio 2006, Idriss and Boulanger 2008).

73 The first objective of this study is to evaluate excess pore pressure generation as a function of
74 the following soil characteristics; soil index properties (e.g., FC, Atterberg limits, silt and clay
75 contents, interfine void ratio, and gradation) and stress history (overconsolidation ratio, OCR).
76 Data from cyclic Direct Simple Shear (CDSS) tests on intact samples from six engineering project
77 sites in Oregon and Washington has been evaluated. The soils were obtained from different

78 coastal marine environments and fluvial depositional environments, including riverine and
79 estuarine/tidal. The second objective of the study is to provide calibrated Vucetic and Dobry model
80 (Vucetic and Dobry 1986; Matasović 1993; Matasović and Vucetic 1993) parameters (hereafter
81 referred to as V&D) for the tests presented in this paper. The V&D model is one of several
82 available constitutive models to simulate cyclic pore pressures in soils and is a focus of this study
83 because of its widespread use in effective-stress site response analysis tools, and because it
84 provides a means to evaluate excess pore pressure tendencies with varying cyclic shear strain
85 and loading cycles. The V&D model parameters developed for silt soils in this study are compared
86 to model parameters presented for sand soils in other studies to highlight the difference between
87 excess pore pressure generation in sands and low-plasticity silts. Finally, a set of predictive
88 equations are provided as a benchmark for practitioners to use when selecting constitutive model
89 parameters for silt-rich soils.

90 **2 DATA USED IN THIS STUDY**

91 **2.1 Soil Classification & Index Properties**

92 The dataset presented in this study includes 35 strain-controlled constant volume direct simple
93 shear (CDSS) tests and a series of field shaking tests using truck-mounted shakers from the
94 NHERI@UTexas facility at the University of Texas at Austin. Additionally, data from six stress-
95 controlled CDSS tests are included where the data were analyzed by McCullough et al. (2009)
96 using procedures by Matasović and Vucetic (1993) to interpret pore water pressures at average
97 shear strain amplitudes to be comparable to strain-controlled test data. The tests are performed
98 on intact natural soils from six sites characterized as representative of different depositional
99 environments (alluvial, fluvial, and tidal/estuarine). Table 1 lists key soil properties and test
100 parameters.

101 The majority of the soils collected are fine grained and are characterized as low-plasticity silt (ML),
102 low-plasticity clay (CL), or low-plasticity silty clay (CL-ML) based on their USCS classification. The

103 focus in this study is on silt-rich soils with fines content ranging from 54% to 100%, silt content
104 ranging from 47% to 83%, and PI ranging from NP to 16. Additionally, six strain-controlled CDSS
105 tests on sands (SP) and silty sand soils (SM) with FC ranging between 1% and 31% are included
106 from a site in coastal Washington (Table 1 – Project W_01). These tests helped highlight the
107 differences between pore pressure generation tendencies in sands and silts. The plasticity
108 characteristics of the soils evaluated in this study are plotted in Figure 1a. Figure 1b shows that
109 the soils presented in this study are characterized as being susceptible to liquefaction or cyclic
110 softening based on screening methods by Idriss and Boulanger (2008) using the illustration
111 method developed by Armstrong and Malvick (2016). It is important to note that the PI of these
112 natural deposits tends to increase with increasing FC, as shown in Figure 1b. This will be later
113 used to highlight some of the differences between the findings in this study and the results of
114 other studies of sand mixtures that contain a nonplastic silt.

115 **2.2 Cyclic Testing**

116 The CDSS tests were performed under constant-volume conditions and the pore pressures were
117 back-calculated from the change in vertical stress. The cyclic shear strain amplitudes (hereafter
118 referred to as cyclic shear strain) in the strain-controlled CDSS tests ranged from 0.1% to 2%.
119 The cyclic loading in CDSS tests was applied mostly at a frequency of 0.1 Hz except for the tests
120 performed at the University of California at Los Angeles for the tidal/estuarine silt deposits in
121 Washington (Project W_03), in which the loading frequency was varied between 0.01 Hz and 0.1
122 Hz. The field shaking tests (Project O_24) by Stokoe et al. (2020) were performed with a loading
123 frequency from the truck shakers of 10 Hz. Various studies have shown the strain rate effects
124 (frequency of loading) on the cyclic resistance and porewater pressure buildup in fine-grained
125 soils. For example, Mortezaie and Vucetic (2013) showed that cyclic porewater pressures
126 consistently increase as the loading frequency is decreased. Therefore, the few data points from
127 Projects W_03 and O_24 where the loading frequencies were different than 0.1 Hz used in the

128 rest of the dataset might be affected by the strain rate effects; however, the conclusions and
129 overall trends are not believed to be affected by these data points. In most cases, the CDSS data
130 were supplemented with bender element shear wave velocity (V_s) measurements performed after
131 consolidation and immediately prior to cyclic loading. The specimens in the CDSS tests were
132 consolidated to a vertical effective stress that was slightly larger than the in-situ vertical effective
133 stress to reduce the effect of sample disturbance (a factor of 1.2 for specimens in Projects W_01
134 and O_01 and factors ranging between 1 and 3.8 for other projects in this database). The field
135 shaking included crosshole V_s measurements prior to cyclic loading.

136 **2.3 Sample Quality Assessment**

137 Several approaches were used to evaluate sample quality on intact specimens. A summary of
138 the available data and sample quality assessment is provided in Table 2. Detailed descriptions of
139 sample quality assessment for different projects and methods used are provided in Appendix A.
140 Overall, the available data from projects O_15, W_01, and W_08 indicate that sample disturbance
141 was minimized. There are no available data to evaluate the disturbance of samples tested for
142 project W_03, however, the project's data report details that Shelby tube sampling was performed
143 with mud rotary drilling and an Osterberg sampler, where these approaches are considered to
144 reduce sample disturbance of fine-grained soils. Samples from O_01 are considered poor quality
145 which likely impacts the laboratory-characterized cyclic behavior.

146 **3 CORRELATIONS BETWEEN CYCLICALLY INDUCED PORE PRESSURES AND SOIL** 147 **INDEX PROPERTIES**

148 **3.1 Effects of Gradation, Plasticity, Void Ratio, and Shear Wave Velocity on Excess** 149 **Pore Pressures**

150 Figure 2 shows the variation of cyclically induced porewater pressure ratio with the number of
151 uniform loading cycles at a constant cyclic shear strain of $\gamma_c = 0.1\%$ —where the porewater
152 pressure ratio is defined as the residual excess porewater pressure at the end of each loading

153 cycle normalized by the initial vertical stress prior to cyclic loading (i.e., $R_u = \Delta u / \sigma'_{vo}$). The trend
154 shows an increasing porewater pressure ratio with the number of cycles. The sand material (SP)
155 generated significantly larger pore pressures compared to those of fine-grained materials (ML,
156 CL, and CL-ML). The variation of R_u and various soil properties are investigated for silt-rich soils
157 in the next section by comparing the R_u values at 30 cycles ($N = 30$). The 30th cycle is selected
158 only as a reference since, in most tests, the R_u values start to plateau at about 30 cycles. It is
159 worth noting that a cycle number ranging between 15 to 30 is typically used in laboratory tests to
160 represent the equivalent number of cycles for a magnitude 7.5 earthquake loading for sand-like
161 and clay-like soils (Idriss and Boulanger 2008).

162 Figure 3 shows the possible correlations, or lack thereof, between R_u at a cyclic shear strain of γ_c
163 = 0.1% after 30 loading cycles with various soil properties. These soil properties are selected
164 based on commonly used screening methods that adopt different combinations of soil properties
165 (e.g., FC, silt content, clay content, PI, liquid limit (LL), ratio of water content to LL (w_c/LL), interfine
166 contact void ratio, and V_s) as indicators to assess the potential for liquefaction and cyclic softening
167 in silts (e.g., Wang, 1979, Ishihara 1993, Youd 1998, Polito and Martin 2001, Andrus and Stokoe
168 2000, Seed et al. 2003, Wang et al. 2006, Boulanger and Idriss 2006, Bray and Sancio 2006, and
169 Thevanayagam 2007). However, it is important to note that the trends shown in Figure 3 present
170 the development of R_u with cyclic loading at low to moderate shear strains (e.g. $\gamma=0.1\%$), which
171 is not directly comparable to liquefaction triggering correlations that are based on high levels of
172 pore pressures (i.e. $R_u=100\%$) and/or large shear strains (i.e. $\gamma=3\%$).

173 The variation between R_u and FC in Figure 3a illustrates that for soils with $FC>30\%$, the excess
174 pore pressure decreases as FC increases. A similar decreasing trend is observed between R_u
175 and the silt content (i.e., particle size between 0.075 mm and 0.005 mm) and clay content (i.e.,
176 particle size smaller than 0.005 mm) as shown in Figures 3b and 3c, respectively. It is speculated
177 that the decreasing trend between R_u and fines/silt/clay content for the natural silts in this study

178 is related to other fundamental soil characteristics such as soil plasticity. The plot presented in
179 Figure 3d shows a decreasing trend between R_u and PI. The NP soils are plotted at PI = 0;
180 however, due to uncertainties in measuring Atterberg limits for soils with very low plasticity, their
181 PI values could be somewhat larger (up to PI ~4). The variations of R_u with LL and w_c/LL are
182 shown in Fig. 3e and Fig. 3f, respectively (excluding the two NP soils). These two variables do
183 not appear to have an effect on R_u for the range of data in this study with LL>27 and $w_c/LL>0.99$.
184 Figure 3g shows an increasing trend between R_u and interfine contact void ratio (e_f). e_f is defined
185 based on the global void ratio (e) and FC using the equation below and has been shown by some
186 studies to relate to liquefaction resistance of soil mixtures where the fine grain contact dominates
187 the cyclic response (e.g., Thevanayagam 2007):

$$e_f = \frac{e}{FC} \quad (1)$$

188 Figure 3h shows the lack of strong correlation between R_u and $V_{s,lab}$ for fine-grained soils data in
189 this study. Some studies have shown that the grain size distribution of sand soils affects their
190 tendency to develop cyclic excess pore pressures. For example, Li (2013) showed that excess
191 pore pressures increase with an increasing coefficient of uniformity (C_u) for Houston Sand.
192 Similarly, Mei et al. (2018) calibrated V&D model parameters for different sands and showed that
193 Parameter F in the V&D model increases with C_u , indicating an increasing tendency to develop
194 excess pore pressures, as addressed in Section 4. In contrast, the data for silt-rich soils used in
195 this study show a decreasing trend between R_u and C_u , as shown in Figure 3i. While some of the
196 soil properties plotted in Figure 3 serve as indicators for decreasing or increasing trends in R_u , no
197 single soil property was found to explain all aspects of the observed experimental data. This
198 observation may be attributed to the inherent variabilities in characteristics of natural soils not
199 captured using the soil parameters applied in Figure 3 (e.g., grain shape, inclusion of biogenic
200 grains, fabric, aging), and the sampling and testing procedures performed in different projects.

201 The relationships between R_u and various soil properties were evaluated at larger cyclic shear
202 strains as well. Figures 4a and 4b show the variation of R_u with the number of loading cycles for
203 cyclic tests performed at constant shear strains of 0.4% and 1.6%, respectively. The results show
204 similar trends to those observed for the tests at 0.1% shear strain, i.e., the sand material (SP)
205 developed considerably higher R_u as compared to the silts and silty soils, even in the first few
206 cycles of loading. The R_u values generally decrease as the PI and FC increase in silts and silty
207 soils (SM, ML, CL). Figures 5a and 5b show R_u for the tests that reached 30 uniform loading
208 cycles at constant shear strains of 0.4% and 1.6% with respect to PI. While the R_u values appear
209 to decrease with increasing PI, the correlation becomes less strong at larger shear strains as the
210 R_u values appear to approach their theoretical maximum value of 100%. The data points
211 corresponding to the fluvial soils with PI of 10 and FC of 60% from Tacoma, Washington (Project
212 W_08) produced noticeably smaller R_u values compared to other specimens from the same soil
213 unit and other soils with similar PI. It is speculated that these samples were slightly
214 overconsolidated, as they were obtained from relatively shallow depths (5 m). The effect of
215 overconsolidation and stress history on porewater pressure generation is discussed in the next
216 section. The scatter in data highlights the importance of accounting for the inherent variability in
217 the estimated pore pressures due to uncertainties in soil properties (e.g., PI and OCR).

218 **3.2 Effects of Stress History on Excess Pore Pressures**

219 The tests performed on overconsolidated (OC) samples exhibited noticeably smaller porewater
220 pressures compared to normally consolidated samples (NC). The results shown in Figure 6 were
221 obtained from nine strain-controlled CDSS tests performed on Willamette Silt samples from
222 Project O_15 with relatively similar plasticity (PI ranging from 5 to 9). The samples were first
223 consolidated to a confining stress larger than their preconsolidation stress and then unloaded to
224 a lower stress to produce overconsolidation ratios (OCRs) of 1.5 and 2.5. The specimens
225 prepared at OCR = 2.5 showed negative to negligible R_u values at shear strains of 0.1% and

226 0.4%, and they developed a positive R_u value of 78% at a relatively large shear strain of 2% after
227 60 cycles of loading. This observation is consistent with the findings of other researchers where
228 the cyclic porewater pressure ratios first decreased with the number of loading cycles at small
229 cyclic shear strains (0.74%) and then increased at larger shear strains (1.68%) in OC clays (e.g.,
230 Dobry and Vucetic 1987 and Vucetic 1988). While some differences in R_u values in Figure 6 could
231 be due to small variations in PI (ranging between 5 and 9) the primary reason for significantly
232 different R_u values in this figure is attributed to the differences in OCR.

233 **3.3 Summary of Excess Pore Pressures in NC and OC Silts**

234 Figure 7 summarizes the R_u values from NC and OC tests on intact, natural silt-rich soils in the
235 database used in this study. For consistency, all R_u values are compared for cyclic shear strain
236 of 0.1% after 30 loading cycles. The R_u values are plotted against FC in this figure to enable them
237 to be compared to the results obtained in other strain-controlled tests performed on sands and
238 silty sands. The observed range of R_u values clearly shows the effect of OCR in decreasing
239 cyclically induced pore pressures. Several supplemental data points from this study (SP and SM
240 soils in Project W_01 and ML soils in Project O_24) and other studies (Jana and Stuedlein 2021)
241 that were added to this figure confirm the observed trends between R_u and FC, and R_u and OCR.
242 The field shaking tests on Columbia River Silt (Project O_24) correspond to soils with PI of 13
243 and OCR ranging from 2.1 to 3 for soils at depths ranging from 1.55 m to 2.55 m. The field shaking
244 tests consisted of sequential tests with increasing amplitude. The subset of data presented in this
245 figure corresponds to shaking events that produced shear strain values close to 0.1% (ranging
246 from 0.08% to 0.12%). The field shakings correspond to $N = 36$ cycles at 10 Hz. More details on
247 the field shaking tests are provided in Stokoe et al. (2020) and Preciado et al. (2021). The field
248 shaking tests data fall within the range of observed values from CDSS tests on OC samples. An
249 additional data point from CDSS tests on intact natural alluvial silts from Columbia River in
250 Portland basin with PI = 26 and OCR from 1.8 to 2 by Jana and Stuedlein (2021) is plotted for

251 comparison purposes; this data point also falls within the range observed for the OC specimens
252 in this study. The PI value for every data point is shown to emphasize that the natural soils in this
253 study have different plasticity indices, and this might contribute to the scatter in the data.

254 The decreasing trend between R_u and FC in this study generally agrees with the results of other
255 studies that used reconstituted sand mixtures with non-plastic silt (e.g., Hazirbaba and Rathje
256 2009). The data in this study expand upon these findings by examining natural silts which tend to
257 be less dilative than mixtures composed of crushed silica for non-plastic fines, and intact
258 specimens that maintain some natural soil fabric and cementation. Additionally, the soils
259 examined in this study provide insight into trends of how R_u relates to FC for FC greater than 30%
260 and varying PI and how R_u relates to OCR. The observed trends between R_u and FC, PI, and
261 OCR shown in Figures 3 to 7 are used as a basis for calibrating V&D parameters for silt soils in
262 the next section.

263 **4 CALIBRATION OF V&D MODEL PARAMETERS FOR SILTS**

264 The second objective of this study is to provide calibrated intermediate soil model parameters for
265 the Vucetic and Dobry (1986) strain-based pore pressure model for sand (i.e., the V&D model) to
266 estimate cyclically induced pore pressures at different numbers of uniform loading cycles and at
267 different shear strain levels. The V&D models are commonly used in practice in effective-stress
268 site response analysis using software programs such as DEEPSOIL (Hashash et al. 2020), D-
269 MOD (Matasović and Vucetic 1995) and D-MOD2000 (Matasović and Ordonez 2012). Olson et
270 al. (2020) showed that using the V&D pore-pressure model in combination with the cyclic stress-
271 strain constitutive model of Groholski et al. (2016) was effective for estimating excess pore
272 pressures in effective-stress site response analysis. The model parameters for V&D sand and
273 clay models are primarily provided in the literature for sand and clay materials, e.g., Dobry et al.
274 (1985), Vucetic (1986), Thilakarante and Vucetic (1987), Vucetic and Dobry (1988), Matasović
275 (1993), Matasović and Vucetic (1993), Matasović and Vucetic (1995), and Mei et al. (2018).

276 Despite the wide use of these models in practice, only a few studies have provided model
277 parameters for silts and silty sands, e.g. Thilakarante and Vucetic (1987), McCullough et al.
278 (2009), and Anderson et al. (2010). Due to the scarcity of data on pore pressure generation in
279 silt-rich soils, the V&D model parameters that are developed primarily for sands are often used
280 by practitioners to evaluate the undrained cyclic response and the pore pressure development
281 tendency of silt-rich soils, particularly when the soils are characterized as susceptible to
282 liquefaction or cyclic softening using screening methods such as those in Idriss and Boulanger
283 (2008) and Bray and Sancio (2006). However, using model parameters that are developed for
284 sands tends to result in an overestimation of the pore pressures in silts as shown by Hazirbaba
285 and Rathje (2009), thereby resulting in an over-softening of the dynamic response of silt layers in
286 one-dimensional effective-stress site response analysis.

287 To address this issue, the V&D model parameters in this study are calibrated using strain-
288 controlled tests on primarily intact, natural silts, as described in the previous section. The
289 calibrated V&D model parameters for silts in this study are compared with those reported in the
290 literature for sands to illustrate the differences between pore pressure development tendencies in
291 sands and silts. Correlations between calibrated model parameters and various soil properties
292 are investigated, and a set of predictive models are proposed to estimate V&D model parameters
293 for silts. An evaluation of the effectiveness of the V&D model for predicting pore pressures in silty
294 soils using the proposed predictive equations is also provided. The V&D parameters that are
295 provided in this paper serve as a reference for practitioners in modeling cyclic behavior of low
296 plasticity silts. It is noteworthy that the V&D sand model is one of the many models that are
297 available for strain-based effective-stress site response analysis (e.g., Green et al. 2000). The
298 V&D model is used in this study since it is widely used in engineering practice.

299 **4.1 Calibration Procedures**

300 The V&D model for sands was fit to the lab data presented in this study. The model equation is
301 provided in Equation (2). Details on the model parameters can be found in Dobry et al. (1985),
302 Vucetic and Dobry (1986), Vucetic (1986), Matasović (1993) and Matasović and Vucetic (1993).

$$R_u = \frac{PfNF(\gamma_c - \gamma_{tvp})^s}{1 + fNF(\gamma_c - \gamma_{tvp})^s} \quad (2)$$

303 where R_u is defined as the residual pore pressure ratio after N cycles of loading at a constant
304 shear strain of γ_c . The f value in Eq. (2) accounts for the direction of loading. The objective in this
305 study is to calibrate the model parameters to data from lab tests that were all performed under
306 unidirectional loading; therefore, $f = 1$ was used in this study. Parameters F , s , and P were
307 calibrated based on curve fitting procedures described in Vucetic (1986), Matasović and Vucetic
308 (1993), and Mei et al. (2018). While the P and F parameters reported in this paper are derived
309 from the curve fitting procedures described in the above references, in most cases, s was defined
310 by iterative adjustment to produce the best fit between the measured and predicted pore
311 pressures, as suggested by Matasović and Vucetic (1993). The cyclic threshold shear strain
312 amplitude for volumetric strain (γ_{tvp}) (hereafter referred to as threshold shear strain) was selected
313 using the middle curve proposed by Mortezaie and Vucetic (2016), which will be shown to
314 reasonably envelop the data from this study and other studies on silts.

315 Figure 8 shows an example comparison between lab-measured and model-predicted R_u values
316 for three strain-controlled CDSS tests performed on Willamette Silt samples (Project O_15). The
317 tests were performed at shear strains of $\gamma_c = 0.1\%$, 0.4% , and 1.6% on specimens consolidated
318 to vertical effective stresses of 240 kPa. These specimens had FC of 99%, silt content of 79%,
319 LL of 30, PI of 9, and water contents ranging between 32% and 36%. These samples are
320 characterized as susceptible to liquefaction and/or cyclic softening based on screening
321 procedures often used in practice (e.g., Bray and Sancio 2006, Idriss and Boulanger 2008).
322 Figure 8a shows R_u versus cyclic shear strain for lab data (indicated as symbols) and the

323 calibrated V&D model (indicated as solid lines). Figure 8b shows R_u versus loading cycles from
324 the CDSS tests and the calibrated V&D model. Variability in the trends of measured and predicted
325 R_u with number of loading cycles is noted for each cyclic shear strain amplitude, therefore it is
326 important to note that the V&D model parameters should be selected by the user to target a
327 specific range of loading cycles and/or shear strains based on project-specific seismic demands.
328 For the calibration performed in this study, the calibrated V&D model reasonably captures the
329 excess pore pressures at larger shear strains (i.e. $\gamma_c = 1.6\%$) and generally performs better for
330 loading cycles greater than 5.

331 The calibrated V&D parameters for all the tests and sites in this study, which are listed in Table
332 3, provide a benchmark for the selection of V&D model parameters in project-specific applications.
333 A comparison between the lab-measured and model-predicted R_u values for all tests in this study
334 is presented in Supplemental Appendix B. In the following sections, the potential correlations, or
335 lack thereof, between V&D model parameters (F , s , P , and γ_{tvp}) and other soil properties (OCR,
336 FC, and V_s) are evaluated.

337 **4.2 Variations between F Parameter and Fines Content**

338 Parameter F in the V&D model is the primary variable that controls the tendency for a soil to
339 develop excess pore water pressure during cyclic loading (i.e., larger F values correspond to
340 larger R_u at a given cyclic shear strain). As shown previously in Figures 3 and 7, the soil tendency
341 to develop excess pore pressure decreases as FC increases. Therefore, it is expected that
342 calibrated F parameters should also decrease as FC increases. Figure 9a shows the variation of
343 the calibrated F parameter with FC. Data from this study is supplemented by data from other
344 sandy soils reported in other studies: Banding Sand reported by Dobry et al. (1985), Wildlife Site
345 Sand A and B and Herber Road Site Sand PB and CF reported by Vucetic and Dobry (1988),
346 Santa Monica Beach Sand reported by Matasović and Vucetic (1993), and Owi Island Sand
347 reported by Thilakarante and Vucetic (1987). Several previous studies have shown that the cyclic

348 behavior of a soil mixture transitions from being governed by the coarse fraction to being governed
349 by the fines fraction at FC ranging between 35% and 50% (Polito and Martin 2001,
350 Thevanayagam et al. 2002, Mitchell and Soga 2005). Similarly, Figure 9a illustrates a transition
351 in pore pressure generation tendency (indicated by Parameter F) at FC between 40% and 50%.
352 While the F parameters for sand soils (FC<40% for the data in this figure) range from 0.75 to 10.9
353 (mean $F = 2.3$) the F parameters for silt soils (FC>50%) are significantly smaller and range from
354 0.3 to 1.1 (mean $F_{NC} = 0.7$).

355 The comparison between the calibrated F parameters for sand soils and silt soils suggests, as
356 expected, that the V&D model parameters developed for sands are not suitable for predicting the
357 pore pressure generation in silts. The analysis in this investigation did not show a strong
358 correlation between F and other fundamental soil properties such as PI. Therefore, the trends
359 suggest that a constant value of $F_{NC} = 0.7$ can be considered for NC silt soils with FC>50% until
360 future refinements can be made as more data become available.

361 **4.3 Variations between s Parameter and Fines Content**

362 Parameter s in the V&D sand model affects the slope and curvature of the relationship between
363 pore pressure ratio and cyclic shear strain. The relationship between parameter s and FC for silt
364 data from this study are compared to that of sand data from other studies in Figure 9b. While the
365 s parameter ranges between 1 and 1.8 for sand soils, it is common to use a value of 1 for clean
366 sand with FC < 5% (e.g. Mei et al. 2018). The difference in trends between sand and silt
367 specimens is evident, with data from silt soils in this study (FC greater than 50%) showing s values
368 much larger than 1 (and up to 2) for intact, natural NC specimens. The silt data suggests a slightly
369 increasing trend between parameter s and FC. As a supplementary trend, the relationship
370 between parameter s and FC proposed by Carlton (2014) is also plotted in this figure which
371 confirms an increasing trend between parameter s and FC. This is expected, considering that

372 Carlton's relationship was developed based on data reported in the literature for sands and three
373 data points on silts with FC>50%, which are all included in this study as well.

374 **4.4 Effects of Overconsolidation Ratio on Calibrated F , s , and P Parameters**

375 The effects of stress history (OCR) on the parameters F , s , and P are shown in Figure 10. The
376 plots in this figure include data from a series of tests performed on intact Willamette Silt specimens
377 (Project O_15), where the specimens were consolidated in the lab to OCR values of 1, 1.5, and
378 2.5. The figure also includes data from field shaking tests conducted on Columbia River Silt
379 (Project O_24) with OCR ranging between 2.1 and 3 (corresponding to the depths of embedded
380 pore pressure sensors). Since the shear strains in the field shaking tests were relatively small
381 (<0.25%), curve fitting for the purpose of calibrating V&D parameters could not be fully
382 constrained at large strains; therefore, a range of calibrated parameters were developed that
383 envelop the measured pore pressures (shown with vertical bars in the figure). While the focus in
384 this paper is on intact specimens, supplemental data from a series of tests on reconstituted
385 samples from estuarine/tidal silts (Project W_04) consolidated to OCR of 1.2 are also included in
386 this figure. Overall, the data in these figures show a decreasing trend between F and OCR and
387 an increasing trend between s and OCR. Parameter P in the V&D model defines the maximum
388 R_u at large shear strains and a large number of loading cycles, somewhat comparable to the R_u
389 values shown previously in Figure 5b (which correspond to a cyclic shear strain of 1.6% and $N =$
390 30). The back-calculated P parameter for NC silts ranged between 0.94 and 1.0 and did not show
391 a strong correlation with other soil properties for NC silts. However, as shown in Figure 10c, P
392 exhibited a decreasing trend with OCR for OC silts.

393 **4.5 Variation Between F parameter and Shear Wave Velocity**

394 Carlton (2014) used available data for sand to develop a relationship between F parameter and
395 V_s . Figure 11 provides a comparison of Carlton's equation in estimating the F parameter for silt
396 soils in this study as well as that for sand soils reported by others. The V_s values for the data

397 points in this study were measured using bender elements in the CDSS device. The significant
398 variability in the silt data precludes a reliable best-fit trendline. It is apparent that the correlation
399 seems to be consistently poor for both sand and silt soils. The F parameters for OC soils are well
400 below the estimated values from Carlton's equation. Similar observations were made by Mei et
401 al. (2018) regarding the comparison between Carlton's equation with V_s data for sands. It is also
402 noted that the two sand data points in this study (SP and SM soils from Project W_01) exhibited
403 noticeably larger F values compared to those of silt soils (ML, CL and CL-ML) having similar V_s
404 values. This finding indicates a higher susceptibility to pore pressure generation for sand soils
405 than for silt soils having similar V_s values. It is important to note that the study presented here
406 evaluates the rate of progressive excess pore pressure generation during cyclic loading (using F
407 parameter as a proxy), which is not directly comparable to V_s -based correlations to predict
408 liquefaction triggering of sand defined based on large R_u values ($\sim 100\%$) and/or large shear
409 strains (e.g., Andrus and Stokoe 2000; Baxter et al. 2008).

410 **4.6 Threshold Shear Strain for Cyclic Pore Water Pressure Generation**

411 The threshold shear strain for cyclically induced pore water pressure (γ_{tvp}) (Dobry et al. 1982) is
412 defined as the shear strain below which no noticeable permanent pore pressure is developed with
413 an increasing number of cycles. Dobry and Abdoun (2015) stated that research using lab and
414 field tests show that γ_{tvp} is a robust soil property for sands that is mostly independent of the number
415 of loading cycles, sand type, nonplastic fines content, relative density, depositional method, and
416 the effective confining pressure between 20 kPa to 200 kPa. Vucetic (1994) showed that γ_{tvp}
417 slightly increases with PI for cohesive materials. His proposed range was further confirmed by
418 Hsu and Vucetic (2006) and was slightly updated by Mortezaie and Vucetic (2016) based on data
419 from two reconstituted clay soils. In Figure 12, the γ_{tvp} extracted from field shaking tests (Project
420 O_24) using truck-mounted shakers are plotted against PI. The results for R_u versus shear strains
421 (γ_c) from field cyclic tests are presented in detail in Stokoe et al. (2020) and Preciado et al. (2021)

422 and are included in Appendix C for completeness. For comparison, data from reconstituted clay
423 soils by Mortezaie and Vucetic (2016) and natural intact alluvial plastic silt by Jana and Stuedlein
424 (2021) are also plotted in Figure 12. The recommended range by Mortezaie and Vucetic (2016)
425 reasonably envelops the data points from this study and other studies. Dobry and Abdoun (2015)
426 reported that overconsolidation of sand increases γ_{vp} . While the field shaking data in this study
427 appear to confirm that such trends may also exist for silts, more data is required to reliably
428 investigate this behavior. As a practical approach, it appears reasonable to continue using the
429 range proposed by Mortezaie and Vucetic (2016) in engineering applications.

430 **4.7 Predictive Equations for V&D Model Parameters for Silts**

431 The relationships between V&D model parameters and other soil properties shown in previous
432 plots were used to develop a set of predictive equations to estimate model parameters (i.e., γ_{vp} ,
433 F , s , and P) as a function of PI, FC, and OCR for silt-rich soils. Note that these relationships are
434 developed for low plasticity silts that classify as ML, CL or CL-ML based on the USCS
435 classification system. The range of applicability of these equations include fine-grained soils with
436 FC ranging from 50% to 100%, silt content ranging from 47% to 81%, PI ranging from NP to 16,
437 and OCR ranging from 1 to 2.5. The proposed equations provide an improved means to select
438 model parameters for silts compared to currently available data that is mostly obtained from
439 sands. A useful compilation of available data can be found in the current DEEPSOIL User Manual
440 (Hashash 2020) and the D-MOD2000 User Manual (Matasović and Ordonez 2011). The proposed
441 equations provide insights on clear differences between sands and silty sands (FC<50%) and
442 silts (FC>50%), and the important effects of OCR on the cyclic response of silts. However, some
443 variations in responses could not be explained. These variations are likely due to inherent
444 variability in tests performed on natural intact soils. Future test programs may further investigate
445 this variability. Therefore, the equations provided below are recommended for the sake of
446 bracketing likely ranges of parameters used in preliminary analyses. It is recommended that cyclic

447 tests are performed as part of the project scope when the estimated pore pressures and cyclic
448 softening of soils have a significant influence on design and associated risks.

449 The proposed relationships for V&D model parameters are listed below:

$$\gamma_{tvp}[\%] = 0.01 + PI/900 \quad (3)$$

(based on average of the recommended range by Mortezaie and Vucetic 2016)

$$P = 1.0 \times OCR^{-0.23} \quad (4)$$

$$F_{NC} = 0.7 \text{ (mean value for NC silt)} \quad (5a)$$

$$F_{OC} = F_{NC} \times OCR^{-2.5} \quad (5b)$$

$$s_{NC} = (1 + FC)^{0.1252} \text{ (the relationship proposed by Carlton 2014)} \quad (6a)$$

$$s_{OC} = s_{NC} \times OCR^{0.5} \quad (6b)$$

450

451 The accuracy of the proposed predictive equations for V&D model parameters for silts is
452 evaluated by comparing the predicted and measured R_u values at the same shear strain and
453 number of the loading cycle. In Figure 13a, the measured R_u values are compared to R_u values
454 predicted using the V&D model when the model parameters are calculated using the proposed
455 relationships in this study (Equations (3) to (6)). The R_u values plotted in this figure correspond to
456 35 strain-controlled CDSS tests with shear strains ranging from 0.07% to 2% and number of
457 loading cycles ranging from 1 to 60. The 1:1, 1:2 and 2:1 lines are plotted for reference. The
458 plotted data points are binned into three categories based on their PI to evaluate the potential
459 influence of soil plasticity. R_u values smaller than 0.4 are, on average, underpredicted by the
460 model; R_u values greater than 0.4 are generally overpredicted, but are bounded by the 1:2 and
461 2:1 lines. The model predictions seem to be slightly more accurate for low plasticity silts with $PI < 7$.
462 The scatter in the data is due to two sources of uncertainty: (a) the robustness of the proposed
463 predictive equations in estimating the V&D model parameters, and (b) possible limitations in the
464 applicability of the V&D model, which was originally developed for sand, to the fine-grained low-
465 plasticity silts ($FC \geq 50\%$ and PI ranging from NP to 16) evaluated in this investigation. To
466 differentiate the sources of uncertainty additional comparisons are made between measured and

467 predicted R_u values, using V&D model parameters that are specifically calibrated for each set of
468 lab data (reported in Table 2); these comparisons are shown in Figure 13b. The model is shown
469 to reasonably predict R_u values larger than 0.4. This is expected, considering that the calibration
470 procedure favored test data at larger shear strains and R_u values. This figure demonstrates that
471 the V&D sand model can be effectively applied to fine-grained silts with PI ranging between NP
472 to 16 if calibrated to lab data. The reduction in scatter from Fig. 13a to Fig. 13b highlights the
473 benefit of performing cyclic lab tests to reduce uncertainty.

474 **5 CONCLUDING REMARKS**

475 A series of cyclic shear tests that includes 35 strain-controlled CDSS tests and field shaking tests
476 on low-plastic silts from six different soils were used in this study to (a) evaluate the variation of
477 cyclically induced excess pore pressures with various soil index properties and stress histories,
478 and (b) provide calibrated Vucetic and Dobry (1986) model parameters for these tests. The focus
479 in this study was on fine-grained, silt-rich soils with fines content (FC) ranging from 54% to 100%,
480 silt content ranging from 47% to 83%, and plasticity index (PI) ranging from NP to 16. The
481 evaluation of data in this study provided insights on differences between clean sands and silty
482 sands (FC<50%) and fine-grained silts (FC>50%). The important effects of stress history and
483 overconsolidation on the cyclic response of silts are listed below:

- 484 • R_u values in silts decrease with increasing FC, silt content, and PI and increase with increasing
485 interfine void ratio. These trends were more obvious for tests performed at a cyclic shear strain
486 of 0.1%, but were also observed in tests performed at larger cyclic strains (up to 2%).
- 487 • R_u values for OC silts with OCR ranging between 1.5 to 3 were found to be significantly smaller
488 than those of NC soils with OCR = 1 for cyclic shear strains between 0.1% and 2%.
- 489 • The threshold shear strains for pore pressure generation (γ_{tvp}) were calculated from field
490 shaking tests on silts with PI = 13 and OCR from 2.1 to 3. The values were found to be

491 enveloped by the range proposed by Mortezaie and Vucetic (2016), affirming that the
492 threshold shear strain is a fundamental soil property.

- 493 • The calibrated V&D model parameters for silts were found to be significantly different from
494 those reported in the literature for sands. The F parameter for NC silts ($FC > 50\%$) ranged from
495 0.3 to 1.1 with a mean value of 0.7, while the F parameter for sand ($FC < 50\%$) reported in the
496 literature ranged from 0.7 to 10.9 with a mean value of 2.2.
- 497 • The calibrated V&D model parameters were significantly affected by OCR. The F and P
498 parameters were found to decrease with OCR, while the s parameter increased with OCR.
- 499 • A set of predictive equations were developed to calculate V&D model parameters for low-
500 plastic silts ($FC > 50\%$ and PI between NP and 16) based on data in this study. The predicted
501 and measured R_v values were generally bounded with 1:2 and 2:1 ratios.
- 502 • It was shown that performing strain-controlled cyclic shear tests on silts reduces the
503 uncertainty in calibrating V&D models for design applications.

504 **6 ACKNOWLEDGEMENTS**

505 The authors thank the many individuals and organizations that provided data and support for this
506 study: Jan Six (formerly with the Oregon Department of Transportation), Tony Allen (Washington
507 State Department of Transportation), Scott Schlechter, Jason Bock, and Jack Gordon (GRI Inc.),
508 Don Anderson and Nason McCullough (Jacobs), Park Piao, Sam Sideras, Bill Perkins, and Bob
509 Mitchell (Shannon & Wilson), and Professor Kenneth Stokoe (University of Texas at Austin.)
510 Support for field shaking was provided by Grant No. CMMI-1935670 from the National Science
511 Foundation.

512 **7 REFERENCES**

- 513 Anderson, D. G., Shin, S., & Kramer, S. L. (2011). Nonlinear, Effective-Stress Ground Motion
514 Response Analyses Following AASHTO Specifications for Load and Resistance Factor Design
515 Seismic Bridge Design. *Transp Res Rec*;2251:144–54. <https://doi.org/10.3141/2251-15>
- 516 Andrus, R. D., & Stokoe II, K. H. (2000). Liquefaction resistance of soils from shear-wave
517 velocity. *J Geotech Geoenviron Eng*;126:1015–25. [https://doi.org/10.1061/\(ASCE\)1090-0241\(2000\)126:11\(1015\)](https://doi.org/10.1061/(ASCE)1090-0241(2000)126:11(1015))

519 Armstrong, R. J., & Malvick, E. J. (2016). Practical considerations in the use of liquefaction
520 susceptibility criteria. *Earthq Spectra*;32:1941–50. <https://doi.org/10.1193/071114EQS100R>

521 Baxter, C. D., Bradshaw, A. S., Green, R. A., & Wang, J. H. (2008). Correlation between cyclic
522 resistance and shear-wave velocity for providence silts. *J Geotech Geoenviron Eng*;134:37–
523 46. [https://doi.org/10.1061/\(ASCE\)1090-0241\(2008\)134:1\(37\)](https://doi.org/10.1061/(ASCE)1090-0241(2008)134:1(37))

524 Bray, J. D., & Sancio, R. B. (2006). Assessment of the liquefaction susceptibility of fine-grained
525 soils. *J Geotech Geoenviron Eng*; 132:1165–77. [https://doi.org/10.1061/\(ASCE\)1090-0241\(2006\)132:9\(1165\)](https://doi.org/10.1061/(ASCE)1090-0241(2006)132:9(1165))

527 Carlton, B. (2014). An improved description of the seismic response of sites with high plasticity
528 soils, organic clays, and deep soft soil deposits. PhD Dissertation. University of California,
529 Berkeley

530 CH2M Hill (2008). I-5 Tacoma/Pierce County HOV Program Portland Avenue to Port of Tacoma
531 Project Puyallup River Bridge (BR 5/456) – Site-Specific Seismic Ground Response Analysis
532 using DMOD2000. Prepared for Washington State Department of Transportation Headquarter
533 Geotechnical, April 29, 2008.

534 CH2M Hill (2009). WSDOT General Mark W. Clark Memorial Bridge (532/2) Seismic Response
535 Study XL-2770. Prepared for Washington Department of Transportation Headquarters
536 Geotechnical Branch, February 2009.

537 Dahl, K. R., DeJong, J. T., Boulanger, R. W., Pyke, R., and Wahl, D. (2014). Characterization of
538 an alluvial silt and clay deposit for monotonic, cyclic and post-cyclic behavior. *Can Geotech*
539 *J*;51:432 –40. <https://doi.org/10.1139/cgj-2013-0057>

540 Dahl, K., Boulanger, R. W., & DeJong, J. T. (2018). Trends in experimental data of intermediate
541 soils for evaluating dynamic strength. In: *Proceedings of the 11th US National Conference on*
542 *Earthquake Engineering*. Los Angeles, Calif.: Earthquake Engineering Research Institute,
543 June.

544 DeJong, J. T., Krage, C. P., Albin, B. M., & DeGroot, D. J. (2018). Work-based framework for
545 sample quality evaluation of low plasticity soils. *J. Geotech Geoenviron Eng*; 144(10),
546 04018074.

547 Dobry, R., Ladd, R. S., Yokel, F. Y., Chung, R. M., & Powell, D. (1982). Prediction of pore water
548 pressure buildup and liquefaction of sands during earthquakes by the cyclic strain method (Vol.
549 138, p. 150). Gaithersburg, MD: National Bureau of Standards.

550 Dobry, R., Pierce, W. G., Dyvik, R., Thomas, G. E., & Ladd, R. S. (1985). Pore pressure model
551 for cyclic straining of sand. Troy, New York: Rensselaer Polytechnic Institute.

552 Dobry, R. and Vucetic, M., (1987). State-of-the-Art Report: Dynamic Properties and Response of
553 Soft Clay Deposits. *Proceedings of the International Symposium on Geotechnical Engineering*
554 *of Soft Soils*, Mexico City, Editors: Mendoza, M.J. and Montanez, L, Publisher: Sociedad
555 Mexicana de Mecanica de Suelos, Mexico City, August, Vol. 2, pp. 51-87

556 Dobry, R., & Abdoun, T. (2015). Cyclic shear strain needed for liquefaction triggering and
557 assessment of overburden pressure factor $k \sigma$. *J Geotech Geoenviron Eng*;141:04015047.
558 [https://doi.org/10.1061/\(ASCE\)GT.1943-5606.0001342](https://doi.org/10.1061/(ASCE)GT.1943-5606.0001342)

559 Green, R.A., Mitchell, J.K. and Polito, C.P. (2000). An Energy-Based Pore Pressure Generation
560 Model for Cohesionless Soils, *Proceedings: John Booker Memorial Symposium*, Melbourne,
561 Australia, November 16-17, 2000.

562 GRI (2012). Cyclic Testing Data Report ODOT OR!8: Newberg-Dundee Bypass. Prepared for
563 ODOT Region 2 Bridge/Geo/Hydro Unit, October 3, 2012.

564 Hashash, Y.M.A., Musgrove, M.I., Harmon, J.A., Ilhan, O., Xing, G., Numanoglu, O., Groholski,
565 D.R., Phillips, C.A., and Park, D. (2020). DEEPSOIL 7.0, User Manual. Urbana, IL, Board of
566 Trustees of University of Illinois at Urbana-Champaign.

567 Hazirbaba, K., & Rathje, E. M. (2009). Pore pressure generation of silty sands due to induced
568 cyclic shear strains. *J Geotech Geoenviron Eng*;135:1892–1905. [https://doi.org/10.1061/\(ASCE\)GT.1943-5606.0000147](https://doi.org/10.1061/(ASCE)GT.1943-5606.0000147)

569

570 Hsu, C. C., & Vucetic, M. (2006). Threshold shear strain for cyclic pore-water pressure in cohesive
571 soils. *J Geotech Geoenviron Eng*;132:1325–35. [https://doi.org/10.1061/\(ASCE\)1090-](https://doi.org/10.1061/(ASCE)1090-)
572 0241(2006)132:10(1325)

573 Idriss, I. M., & Boulanger, R. W. (2008). *Soil liquefaction during earthquakes*. 2nd Ed. Oakland,
574 Calif.: Earthquake Engineering Research Institute.

575 Jana, A., & Stuedlein, A. W. (2021). Monotonic, Cyclic, and Postcyclic Responses of an Alluvial
576 Plastic Silt Deposit. *J Geotech Geoenviron Eng*;147: 04020174. [https://doi.org/](https://doi.org/10.1061/(ASCE)GT.1943-5606.0002462)
577 10.1061/(ASCE)GT.1943-5606.0002462

578 Koester, J. P. (1994). The influence of fine type and content on cyclic resistance. In: *Ground*
579 *failures under seismic conditions (Geotech. Spec. Publ. No. 44)*. New York: American Society
580 of Civil Engineers; 17–33.

581 Lunne, T., Berre, T., Andersen, K. H., Strandvik, S., & Sjursen, M. (2006). Effects of sample
582 disturbance and consolidation procedures on measured shear strength of soft marine
583 Norwegian clays. *Canadian Geotechnical Journal*, 43(7), 726-750.

584 Matasović N. (1993). *Seismic response of composite horizontally-layered soil deposits*, Ph.D.
585 Thesis, Los Angeles, Calif.: University of California, Los Angeles.

586 Matasović, N. and Vucetic M. (1993). *Seismic Response of Composite Horizontally-Layered Soil*
587 *Deposits*, UCLA Research Report No. ENG-93-182, Civil Engineering Department, University
588 of California, Los Angeles, CA, March, 452 p.

589 Matasovic, N. and Vucetic, M. (1995). *Seismic Response of Soil Deposits Composed of Fully-*
590 *Saturated Clay and Sand Layers*, Proceedings of the 1st International Conference on
591 Geotechnical Earthquake Engineering, Tokyo, Japan, Editor: Ishihara, K., Publisher: A.A.
592 Balkema, Rotterdam/Brookfield, Vol. I, pp. 611-616. November. Matasović, N., & Ordonez, G.
593 (2012). D-MOD2000—A computer program for seismic site response analysis of horizontally
594 layered soil deposits, earthfill dams and solid waste landfills: User’s manual. Lacey, Wash.:
595 Geomotions, LLC. Available at [http://www.geomotions.com/Download/D-](http://www.geomotions.com/Download/D-MOD2000Manual.pdf)
596 MOD2000Manual.pdf

597 Matasović, N. and Vucetic, M. (1995). Generalized cyclic-degradation-pore-pressure generation
598 model for clays. *J Geotech Eng* 121:33–42. [https://doi.org/10.1061/\(ASCE\)0733-](https://doi.org/10.1061/(ASCE)0733-)
599 9410(1995)121:1(33)

600 McCullough, N. J., Hoffman, B., Takasumi, D. L., Anderson, D. G., & Dickenson, S. E. (2009).
601 *Seismic Site Response for an LNG Facility—Analyses and Lessons Learned*. In *TCLEE 2009:*
602 *Lifeline Earthquake Engineering in a Multihazard Environment*; pp. 1–12.
603 [https://doi.org/10.1061/41050\(357\)111](https://doi.org/10.1061/41050(357)111)

604 Mei, X., Olson, S.M. and Hashash, Y.M. (2018). Empirical porewater pressure generation model
605 parameters in 1-D seismic site response analysis. *Soil Dyn Earthq Eng* 114:563–7.
606 <https://doi.org/10.1016/j.soildyn.2018.07.011>

607 Mitchell, J. K., & Soga, K. (2005). *Fundamentals of Soil Behavior*. 3rd Ed. New York: John Wiley
608 & Sons.

609 Mortezaie, A. R., & Vucetic, M. (2013). Effect of frequency and vertical stress on cyclic
610 degradation and pore water pressure in clay in the NGI simple shear device. *Journal of*
611 *Geotechnical and Geoenvironmental Engineering*, 139(10), 1727-1737.

612 Mortezaie, A., & Vucetic, M. (2016). Threshold shear strains for cyclic degradation and cyclic pore
613 water pressure generation in two clays. *J Geotech Geoenviron Eng*;142:04016007.
614 [https://doi.org/10.1061/\(ASCE\)GT.1943-5606.0001461](https://doi.org/10.1061/(ASCE)GT.1943-5606.0001461)

615 Mousavi, S., & Ghayoomi, M. (2021). Liquefaction mitigation of sands with nonplastic fines via
616 microbial-induced partial saturation. *J Geotech Geoenviron Eng*;147:04020156.
617 [https://doi.org/10.1061/\(ASCE\)GT.1943-5606.0002444](https://doi.org/10.1061/(ASCE)GT.1943-5606.0002444)

618 Polito, C. P., & Martin II, J. R. (2001). Effects of nonplastic fines on the liquefaction resistance of
619 sands. *J Geotech Geoenviron Eng*;127:408–15. [https://doi.org/10.1061/\(ASCE\)1090-](https://doi.org/10.1061/(ASCE)1090-)
620 0241(2001)127:5(408)

621 Preciado, A. M., Sorenson, K., Khosravifar, A., Moug, D., Stokoe, K., Menq, F., & Zhang, B.
622 (2021). Evaluating cyclic loading response of a low plasticity silt with laboratory and field cyclic
623 loading tests. ASCE Lifelines 2021 Conference UCLA. Reston, Va.: American Society of Civil
624 Engineers.

625 Shannon and Wilson, Inc. (2004). Seismic Ground Motion Study Report – SR99: Alaskan Way
626 Viaduct and Seawall Replacement Project. Prepared for Washington State Department of
627 Transportation Urban Corridors Office, October 2004.

628 Shen, C. K., Vrymoed, J. L., and Uyeno, C. K. (1977). The effects of fines on liquefaction of sands.
629 In: Proceedings of the 9th International Conference on Soil Mechanics and Foundation
630 Engineering, Vol. 2. Tokyo, Japan: Japanese Society of Soil Mechanics and Foundation
631 Engineering; pp. 381–5.

632 Stokoe, K.H., Zhang, B., and Menq, F. (2020). Field Assessment of the Microbially Induced
633 Desaturation (MID) Method to Mitigate Liquefaction in Silty Soils with Plasticity. GEotechnical
634 Engineering Report GR20-04, Geotechnical Engineering Center, The University of Texas at
635 Austin; 58 p.

636 Tan, T.S., Lee, F.H., Chong, P.T., and Tanaka, H. (2002). Effect of sampling disturbance on
637 properties of Singapore clay. *Journal of Geotechnical and Geoenvironmental Engineering*,
638 128(11): 898-906.

639 Thevanayagam, S., Shenthan, T., Mohan, S., & Liang, J. (2002). Undrained fragility of clean
640 sands, silty sands, and sandy silts. *J Geotech Geoenviron Eng*;128:849–59.
641 [https://doi.org/10.1061/\(ASCE\)1090-0241\(2002\)128:10\(849\)](https://doi.org/10.1061/(ASCE)1090-0241(2002)128:10(849))

642 Thevanayagam, S. (2007). Intergrain contact density indices for granular mixes—I:
643 Framework. *Earthq Eng Eng Vib*;6:123. <https://doi.org/10.1007/s11803-007-0705-7>

644 Thilakarathne, V. and Vucetic, M. (1987). Class-A Prediction of Accelerations and Seismic Pore
645 Pressures at the Owi Island Site during Oct. 4 1985 Earthquake in Tokyo Bay-Part I. Research
646 Report, Civ. Eng. Dept., Potsdam, NY: Clarkson Univ.; 60 p.

647 Troncoso, J. H., and Verdugo, R. (1985). Silt content and dynamic behavior of tailing sands.
648 Proceedings of the 12th International Conference on Soil Mechanics and Foundations
649 Engineering; pp. 1311–14.

650 Vaid, Y. P. (1994). Liquefaction of silty soils. In: Prakas S, Dakoulas, P (Eds.) Ground failures
651 under seismic conditions. Reston, Va.: ASCE; October, pp. 1–16

652 Vucetic, M. (1986). Pore Pressure Buildup and Liquefaction at Level Sandy Sites During
653 Earthquakes (California, Japan). PhD dissertation. Troy, NY: Rensselaer Polytechnic Institute.

654 Vucetic M, Dobry R. (1986). Pore pressure build-up and liquefaction at level sandy sites during
655 earthquakes, Research report CE-86-3. Troy, NY: Rensselaer Polytechnic Institute.

656 Vucetic, M., (1988). Normalized Behavior of Offshore Clay Under Uniform Cyclic Loading,
657 *Canadian Geotechnical Journal*, Vol. 25, No. 1, pp. 33-41

658 Vucetic, M. and Dobry, R. (1988). Cyclic triaxial strain-controlled testing of liquefiable sands.
659 In: RT Donaghe, RC Chaney, ML Silver (Eds.), *Advanced triaxial testing of soil and rock*. West
660 Conshohocken, Pa.: ASTM International; <https://doi.org/10.1520/STP977-EB>

661 Vucetic, M. (1994). Cyclic threshold shear strains in soils. *J Geotech Eng*;120:2208–28.
662 [https://doi.org/10.1061/\(ASCE\)0733-9410\(1994\)120:12\(2208\)](https://doi.org/10.1061/(ASCE)0733-9410(1994)120:12(2208))

663 Wijewickreme, D., Soysa, A., & Verma, P. (2019). Response of natural fine-grained soils for
664 seismic design practice: A collection of research findings from British Columbia, Canada. *Soil
665 Dyn Earthq Eng* 124, 280–96. <https://doi.org/10.1016/j.soildyn.2018.04.053>

666 Zapata-Medina, D.G., Finno, R.J., and Vega-Posada, C.A. (2014). “Stress history and sampling
667 disturbance effects on monotonic and cyclic responses of overconsolidated Bootlegger Cove
668 clays.” *Canadian Geotechnical Journal*, 51: 599-609.

Table 1. Cyclic shear tests used in this study

Proj. ID	Project / Location	Soils	Reference	Boring, Sample ID (Depth)	γ_c in Strain-controlled CDSS Tests (%)	Cyclic loading rate (Hz)	D60 / D10 (mm)	Sand / Silt / Clay (%)	FC (%)	PL / LL (PI)	USCS Class.	Natural water content (%)	Void ratio	Consol. stress (kPa) / Vert. effective stress prior to cyclic loading (kPa) / OCR	V_s (m/s)
O_15	ODOT SR 18 Newberg-Dundee By-Pass / Oregon	Willamette Silt / Missoula Flood FF	GRI (2012)	B86, U3 (4.6 m)	0.1, 0.4, 1.6	0.1	0.009 / 0.001	0 / 64 / 36	100	23 / 39 (16)	CL	37.9 - 43.1	1.02 - 1.16	240 / 240 / 1	243
				B153, U5 (9.1 m)	0.1, 0.4, 1.6	0.1	0.011 / 0.0005	1 / 79 / 20	99	21 / 30 (9)	CL	32.4 - 36.3	0.88 - 0.98	240 / 240 / 1	350
				B153, U4 (6.1 m)	0.1, 0.4, 1.6	0.1	0.085 / 0.01	46 / 49 / 5	54	28 / 33 (5)	ML	33.3 - 35.3	0.90 - 0.95	360 / 240 / 1.5	497
				B86, U4 (6.1 m)	0.1, 0.4, 2	0.1	0.018 / 0.0015	3 / 77 / 20	97	24 / 30 (6)	ML	32.8 - 35	0.89 - 0.96	600 / 240 / 2.5	802
W_01	WS SR-532, General Mark W. Clark Bridge / Stanwood, WA	Tidal Silt / Marine Estuarine	Anderson et al. (2011); CH2M Hill (2009)	GMWC-1C-08, ST-2 (10.4 m)	0.1, 0.7	0.1	0.075 / 0.007	39 / 53 / 8	61	23 / 31 (8)	ML	32.3	0.88	144 / 144 / 1 158 / 158 / 1	256 – 282
				GMWC-1A-08, ST-5 (26.5 m)	0.1, 0.7	0.1	0.015 / 0.001	13 / 63 / 24	87	22 / 32 (10)	ML	33	0.71	321 / 321 / 1 350 / 350 / 1	572 – 623
				GMWC-1A-08, ST-1 (15.2 m)	0.1, 0.4, 1.6	0.1	0.35 / 0.15	99 / 1 / 0	1	NA	SP	23.8	0.75	187 / 187 / 1 201 / 201 / 1 215 / 215 / 1	271
				GMWC-1A-08, ST-4 (24.4 m)	0.1, 0.4, 1.6	0.1	0.112 / 0.04	68 / 31 / 1	32	NA	SM	26.5	0.7	297 / 297 / 1 321 / 321 / 1 350 / 350 / 1	263
O_01	Proposed Oregon LNG Facility / Warrenton, OR	Columbia River Silt	McCullough et al. (2009)	BH-6, 40-ST (75.6 m)	3 stress-controlled CDSS *	0.1	NA	1 / 81 / 18	99	25 / 37 (12)	ML	37.3	0.97	800 / 800 / 1	331
				BH-10, 26-ST (40 m)	3 stress-controlled CDSS *	0.1	NA	27 / 67 / 6	73	26 / 36 (10)	ML	33.4 - 34.1	0.89 - 0.91	400 / 400 / 1	311
W_03	WS SR-99, Alaskan Way Viaduct / Seattle, WA	Tidal Silt / Marine Estuarine	Shannon and Wilson (2004)	SDC-001, S-18 (21.6 m)	0.29	0.01 to 0.05	0.06 / 0.004	28 / 66 / 6	72	NP	ML	38.4	0.879	200 / 200 / 1	NA
				SDC-001, S-24 (26.2 m)	0.1	0.01 to 0.1	0.1 / 0.006	46 / 48 / 6	54	23 / 28 (5)	ML	35.6	0.825	223 / 223 / 1	NA
				SDC-001, S-24 (26.2 m)	0.075	0.05 to 0.1	0.06 / 0.002	29 / 66 / 5	71	NP	ML	35.2	0.781	400 / 400 / 1	NA
				SDC-002, S-19 (15.8 m)	0.165	0.05 to 0.1	0.065 / 0.004	37 / 60 / 3	63	NP	ML	38.7	0.957	150 / 150 / 1	NA
W_08	I-5 Puyallup River Bridge / Tacoma, WA	Fluvial Silt	CH2M Hill (2008)	5/456-H-19vwp, ST-4 (4.9 m)	0.1, 0.4, 1.6	0.1	0.07 / 0.003	39 / 48 / 13	61	33 / 43 (10)	ML	42.6	1.14	52 / 52 / 1	117
				WR-12-H-1p-08, ST-16 (20.4 m)	0.1, 0.4, 1.6	0.1	0.09 / 0.009	46 / 47 / 7	54	NP	ML	24.8	0.66	220 / 220 / 1	212
				WR-12-H-1p-08, ST-20 (25.6 m)	0.1, 0.4, 1.6	0.1	0.055 / 0.004	23 / 66 / 11	77	21 / 27 (6)	CL-ML	31.7	0.82	480 / 480 / 1	250
O_24	Sunderland / Portland, OR	Columbia River Silt	Stokoe et al. (2020); Preciado et al. (2021) **	TREX-1P (1.55 m)	0.001 to 0.142	10	NA	10 / 70 / 20	90	25 / 38 (13)	ML	39.5	1.15	92 / 44 / 2.1	92
				TREX-2P (1.75 m)	0.001 to 0.246	10	NA	10 / 70 / 20	90	25 / 38 (13)	ML	39.5	1.15	96 / 43 / 2.2	92
				TREX-SC7 (2.55 m)	0.001 to 0.185	10	0.015 / 0.001	10 / 70 / 20	90	25 / 38 (13)	ML	39.5	1.15	128 / 42 / 3	116
				TREX-4P (4.55 m)	0.004 to 0.031	10	0.017 / 0.001	5 / 75 / 20	95	31 / 48 (17)	ML	49.5	1.275	110 / 52 / 2.1	100

* Stress-controlled test data reduced to excess pore pressures at average strains by McCullough et al. (2009) based on procedures by Matasović and Vucetic (1993)

** Field shaking. Preconsolidation stress determined from oedometer test, in-situ vertical effective stress includes the weight of truck-mounted shakers (T-Rex)

Table 2. Sample quality evaluation

Project	Boring, Sample ID	$\Delta e/e_c$ sample quality designation ^a	C_r/C_c sample quality rating ^b	$V_{s,lab}/V_{s,in situ}$	Gamma image taken to select intact sample?
O_15:	B86, U3	(1)	High	NA	No
	B153, U5	(2)	High	NA	
	B153, U4	(2)	High	NA	
	B86, U4	(1)	High	NA	
W_01	GMWC-1C-08, ST-2	(2) ^c	NA	1.2	Yes – specimens prepared from intact sections
	GMWC-1A-08, ST-5	(2) ^c	NA	0.8	
	GMWC-1A-08, ST-1	(1) ^c	NA	1.2	
	GMWC-1A-08, ST-4	(2) ^c	NA	1.1	
O_01	BH-6, 40-ST	(4) ^c	NA	1.0	Yes – images indicate some fracturing throughout samples
	BH-10, 26-ST	(3) ^c	NA	1.1	
W_03	SDC-001, S-18	NA	NA	NA	No
	SDC-001, S-24	NA	NA	NA	
	SDC-001, S-24	NA	NA	NA	
	SDC-002, S-19	NA	NA	NA	
W_08	5/456-H-19vwp, ST-4	(2)	NA	0.9	Yes – specimens prepared from intact section
	WR-12-H-1p-08, ST-16	(2)	NA	1.1	
	WR-12-H-1p-08, ST-20	NA	NA	0.9	

^aLunne et al (2006): (1) = very good to excellent, (2) = good to fair, (3) = poor, (4) = very poor

^bDeJong et al. (2018): sample quality ratings are High, Moderate, and Low

^cassessed from change in void ratio during reconsolidation to $1.2\sigma'_{vo}$

Table 3. Calibrated V&D parameters

Project / Soil Unit	Boring, Sample ID (USCS), Soil Properties	f	P	v_{vp}	F	s
O_15: SR18 Newberg-Dundee (Willamette Silt / Missoula Flood FF)	B86, U3 (CL), PI = 16, FC = 100%, OCR = 1, $V_s = 243$ m/s	1	0.94	0.03	1.10	1.90
	B153, U5 (CL), PI = 9, FC = 99%, OCR = 1, $V_s = 350$ m/s	1	0.95	0.020	1.00	2.00
	B153, U4 (ML), PI = 5, FC = 54%, OCR = 1.5, $V_s = 497$ m/s	1	0.94	0.015	0.56	2.20
	B86, U4 (ML), PI = 6, FC = 97%, OCR = 2.5, $V_s = 802$ m/s	1	0.80	0.020	0.04	3.10
W_01: WS SR-532, General Mark W. Clark Bridge (Estuarine/Tidal Silt)	1C-08, ST-2 (ML), PI = 8, FC = 61%, OCR = 1, $V_s = 256-282$ m/s	1	1	0.020	1.05	1.50
	1A-08, ST-5 (ML), PI = 10, FC = 87%, OCR = 1, $V_s = 572-623$ m/s	1	1	0.020	0.90	1.60
	1A-08, ST-1 (SP), PI = NP, FC = 1%, OCR = 1, $V_s = 271$ m/s	1	1	0.015	2.6	1.5
	1A-08, ST-4 (SM), PI = NP, FC = 32%, OCR = 1, $V_s = 263$ m/s	1	1	0.015	1.4	1.6
O_01: Warrenton, OR (Columbia River Silt)	BH-6, 40-ST (ML), PI = 10 to 12, FC = 73% to 99%, OCR = 1, $V_s = 311-331$ m/s	1	1.00	0.060	0.493	1.761
W_03: WS SR-99, Alaskan Way Viaduct (Estuarine/Tidal Silt)	SDC-001, S-18, S-24, SDC-002, S-19 (ML), PI = NP to 5, FC = 54% to 72%, OCR = 1	1	1.00	0.015	0.80	1.60
W_08: I-5/Puyallup River Bridge (Fluvial Silt)	H-19vwp, ST-4 (ML), PI = 10, FC = 61%, OCR = 1, $V_s = 117$ m/s	1	0.80	0.020	0.30	1.30
	H-1p-08, ST-16 (ML), PI = NP, FC = 54%, OCR = 1, $V_s = 212$ m/s	1	1.00	0.015	0.50	1.30
	H-1p-08, ST-20 (CL-ML), PI = 6, FC = 77%, OCR = 1, $V_s = 250$ m/s	1	1.00	0.020	0.30	1.60
W_04: Alaskan Way Viaduct (Estuarine/Tidal Silt)	Reconstituted (ML), OCR = 1.2	1	1	0.015	0.54	2
O_24: Columbia River Silt, Portland, OR (Columbia River Silt)	Field shaking (ML), PI = 13, FC = 90%, OCR = 2.1-3, $V_s = 92-116$ m/s	1	0.81*	0.015	0.02	3
		1	0.81*	0.015	0.2	2.5

* Shear strains from field shaking tests were not large enough to constrain model parameter P . Instead, parameter P was estimated for these tests using the predictive equation shown in Figure 10c.

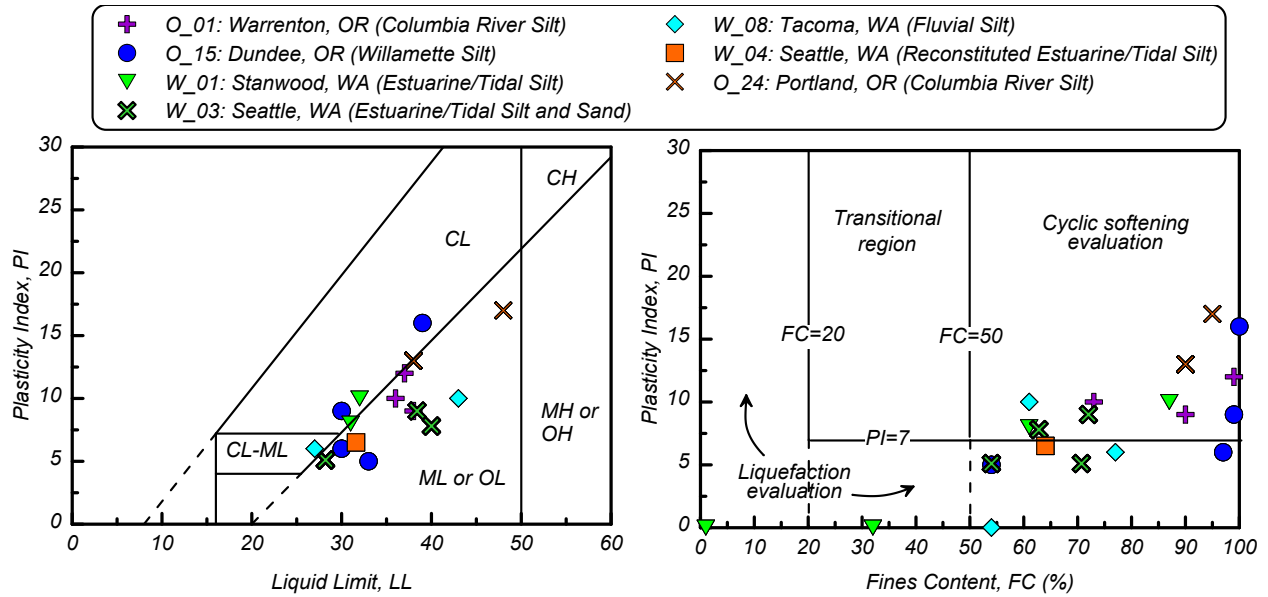


Figure 1: Atterberg limits and fines contents of the soils used in this database and the screening liquefaction and cyclic softening criteria by Idriss and Boulanger (2008) using the illustration by Armstrong and Malvick (2015).

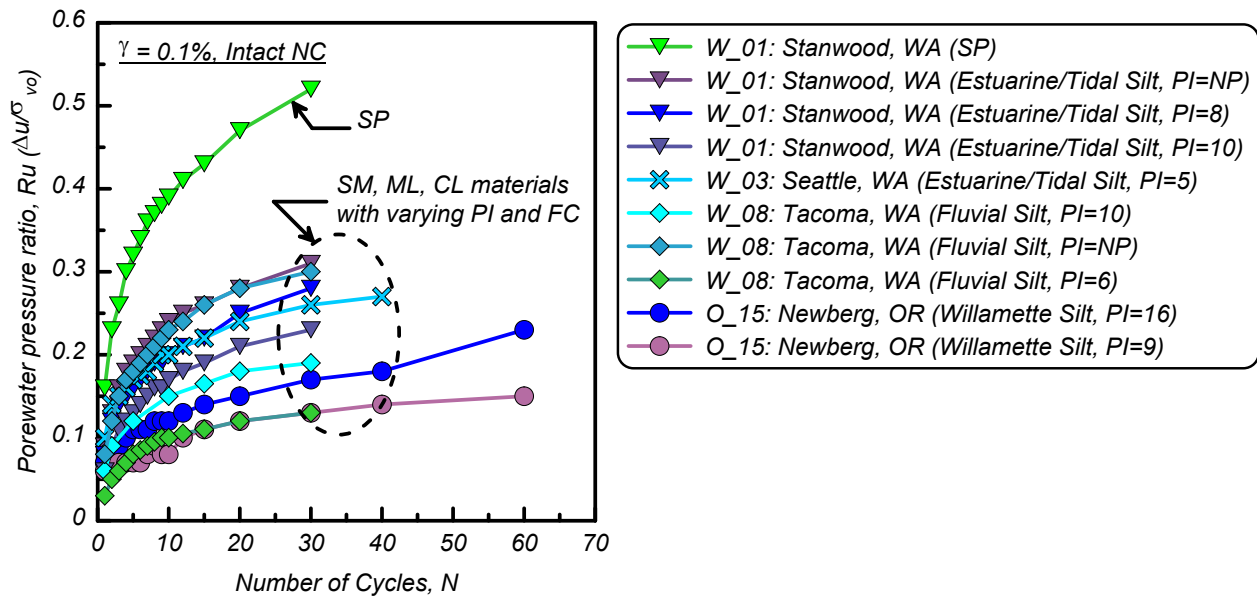


Figure 2: Variation of cyclically induced porewater pressure ratio with the number of uniform loading cycles at a constant cyclic shear strain of $\gamma_c = 0.1\%$ for intact, natural normally consolidated (NC) specimens with different FC (0% to 100%) and PI (NP to 16).

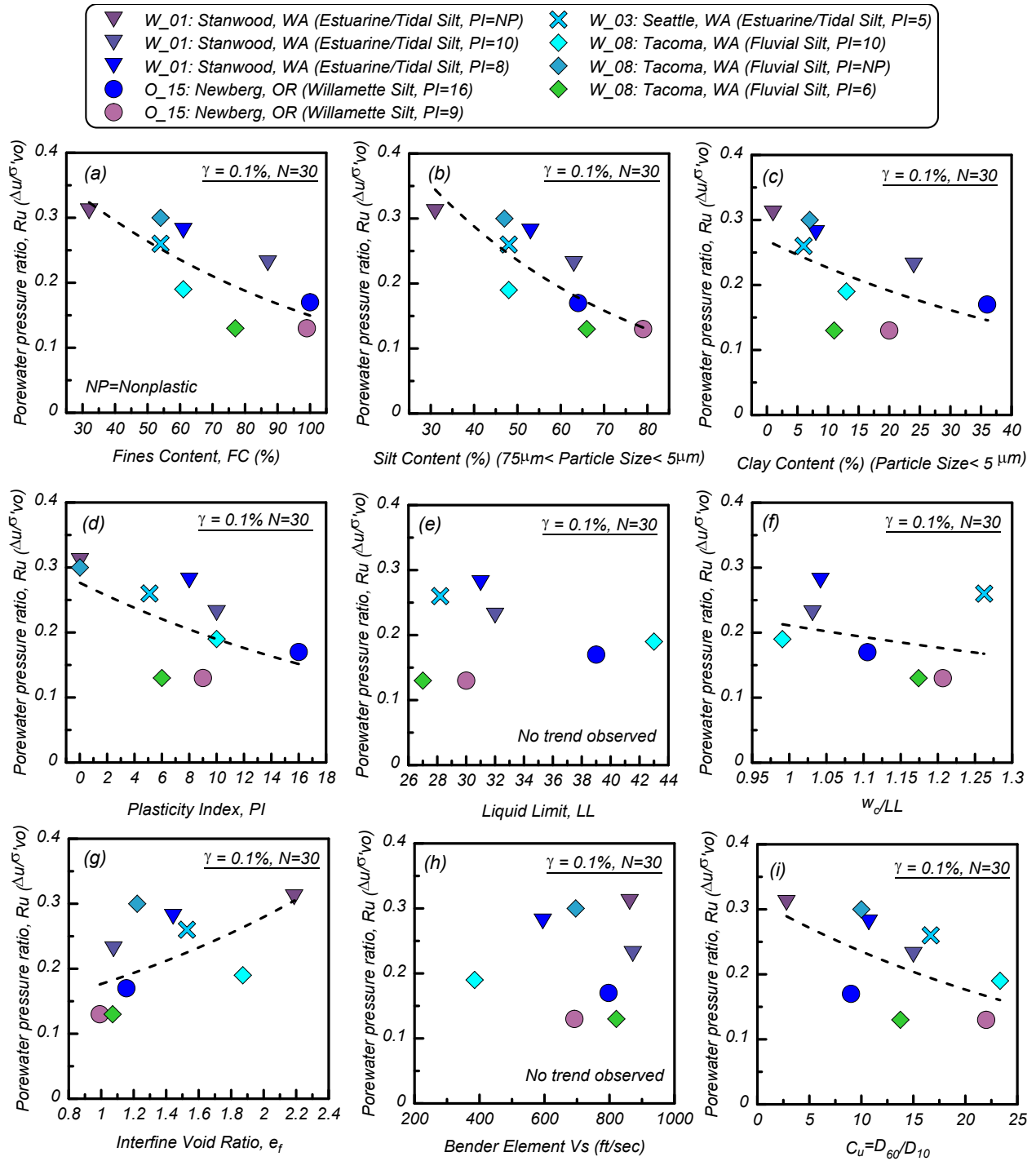


Figure 3: Variation of cyclically-induced porewater pressure ratio after 30 uniform loading cycles at a constant cyclic shear strain of $\gamma_c = 0.1\%$ with (a) fines content, (b) silt content, (c) clay content, (d) plasticity index (PI), (e) liquid limit (LL), (f) water content to liquid limit ratio, (g) interfine void ratio (e_I), (h) bender element shear velocity, and (i) coefficient of uniformity (C_u) for intact, natural normally consolidated (NC) specimens.

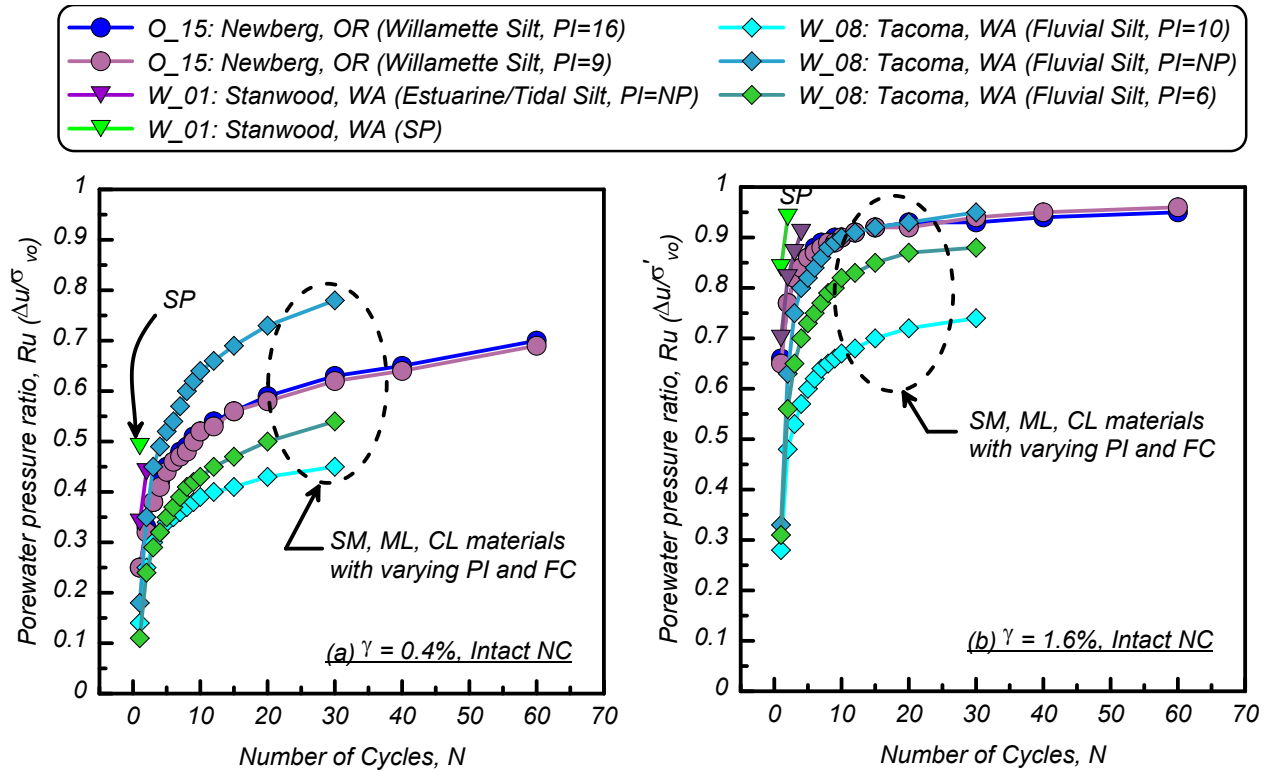


Figure 4: Variation of cyclically induced porewater pressure ratio with number of uniform loading cycles at a constant cyclic shear strain of (a) $\gamma_c = 0.4\%$ and (b) $\gamma_c = 1.6\%$ for intact, natural NC specimens with different FC (0% to 100%) and PI (NP to 16) values.

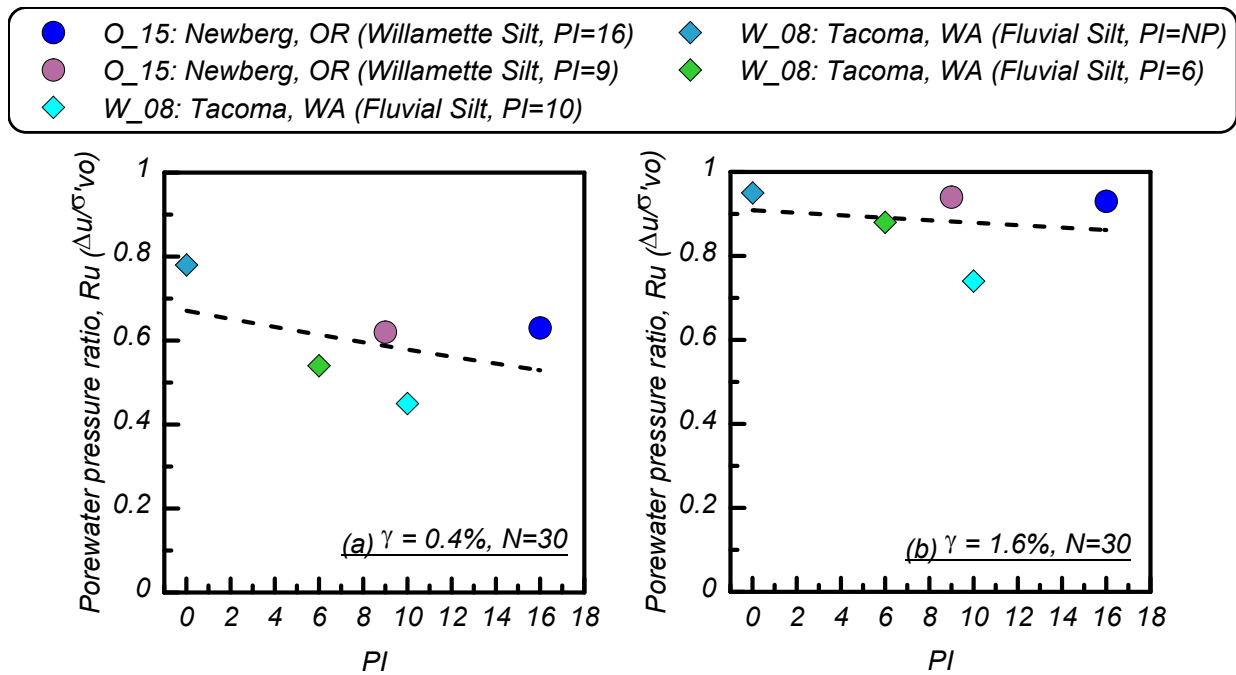


Figure 5: Variation of cyclically induced porewater pressure ratio after 30 uniform loading cycles at a constant cyclic shear strain of (a) $\gamma_c = 0.4\%$ and (b) $\gamma_c = 1.6\%$ with plasticity index for intact, natural, normally consolidated specimens.

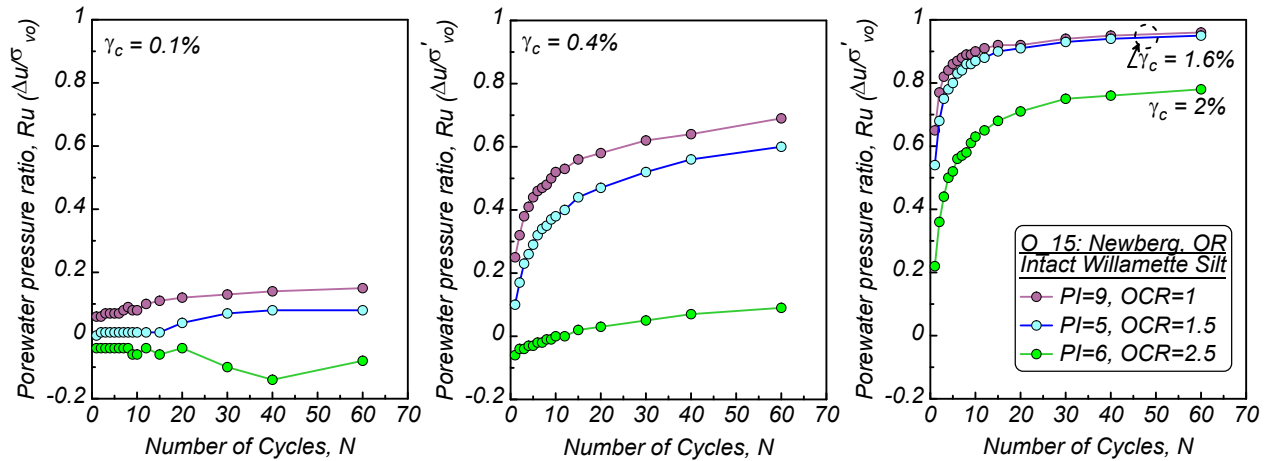


Figure 6: Variation of cyclically-induced porewater pressure ratio with number of uniform loading cycles at a constant cyclic shear strain of (a) $\gamma_c = 0.1\%$ and (b) $\gamma_c = 0.4\%$ and (c) $\gamma_c = 1.6\%$ – 2% for intact, natural NC and OC specimens from Willamette Silt with PIs ranging from 5 to 9 (Project O_15).

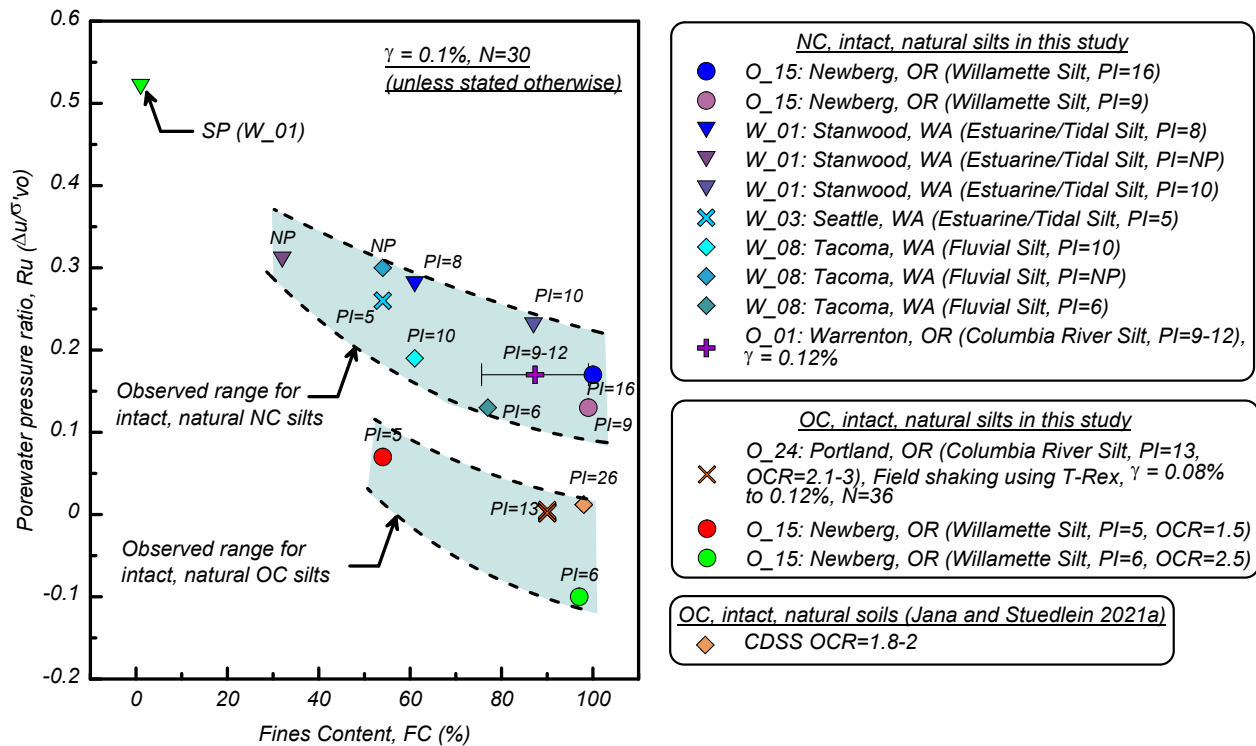


Figure 7: Effect of overconsolidation ratio (OCR) on cyclically-induced porewater pressure ratios at constant cyclic shear strain of $\gamma_c = 0.1\%$ for intact, natural specimens.

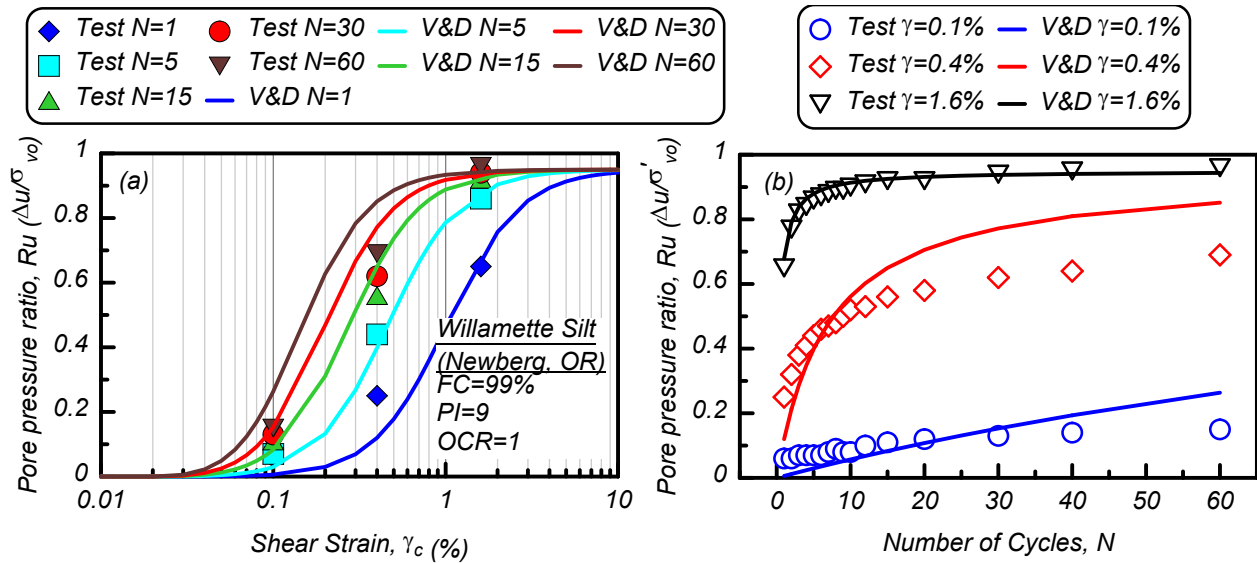


Figure 8: Comparison of measured and predicted R_u from CDSS tests and calibrated V&D model for intact, natural NC samples from Willamette Silt, FC=99%, PI=9 (Project O_15).

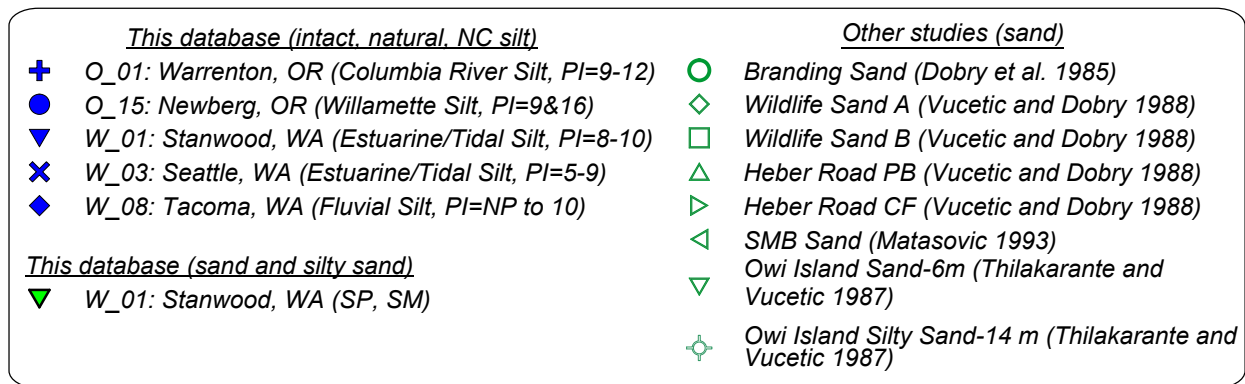


Figure 9: Variation in (a) Parameter F and (b) Parameter s in the V&D model with FC.

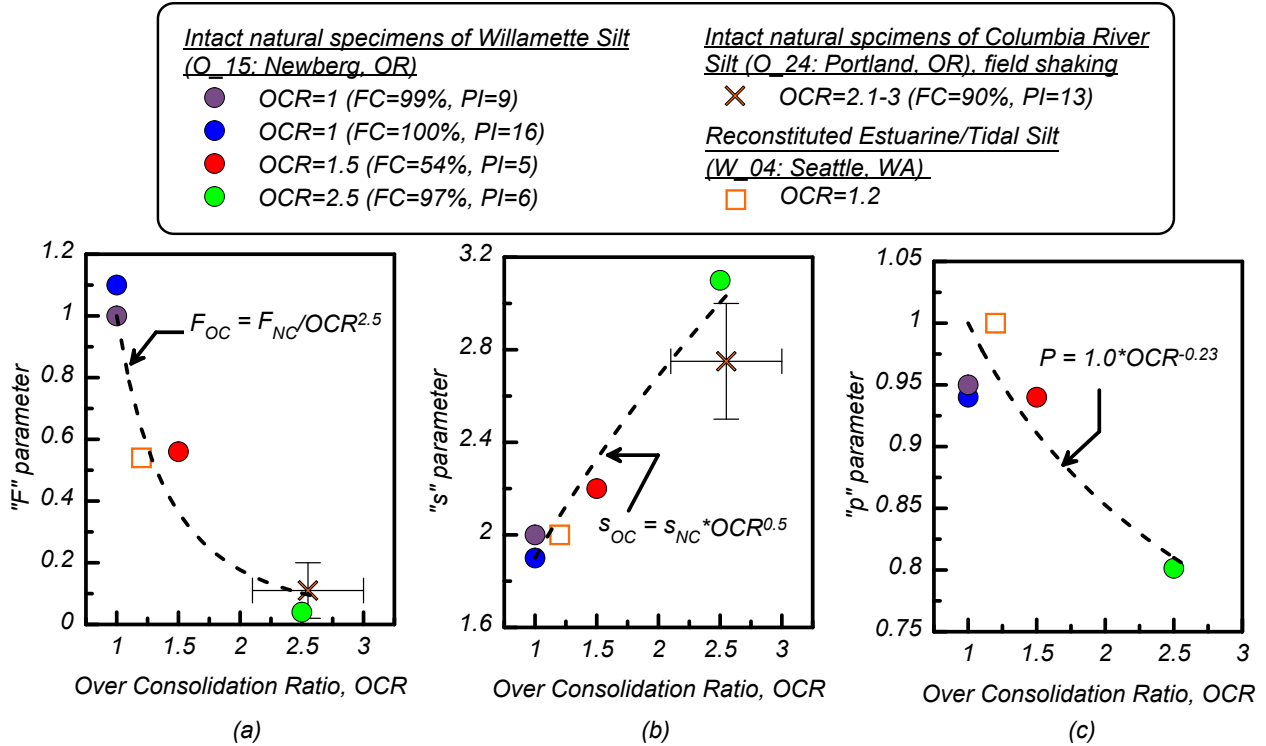


Figure 10: Effects of overconsolidation ratio (OCR) on (a) Parameter F , (b) Parameter s , and (c) Parameter P in the Vucetic and Dobry model.

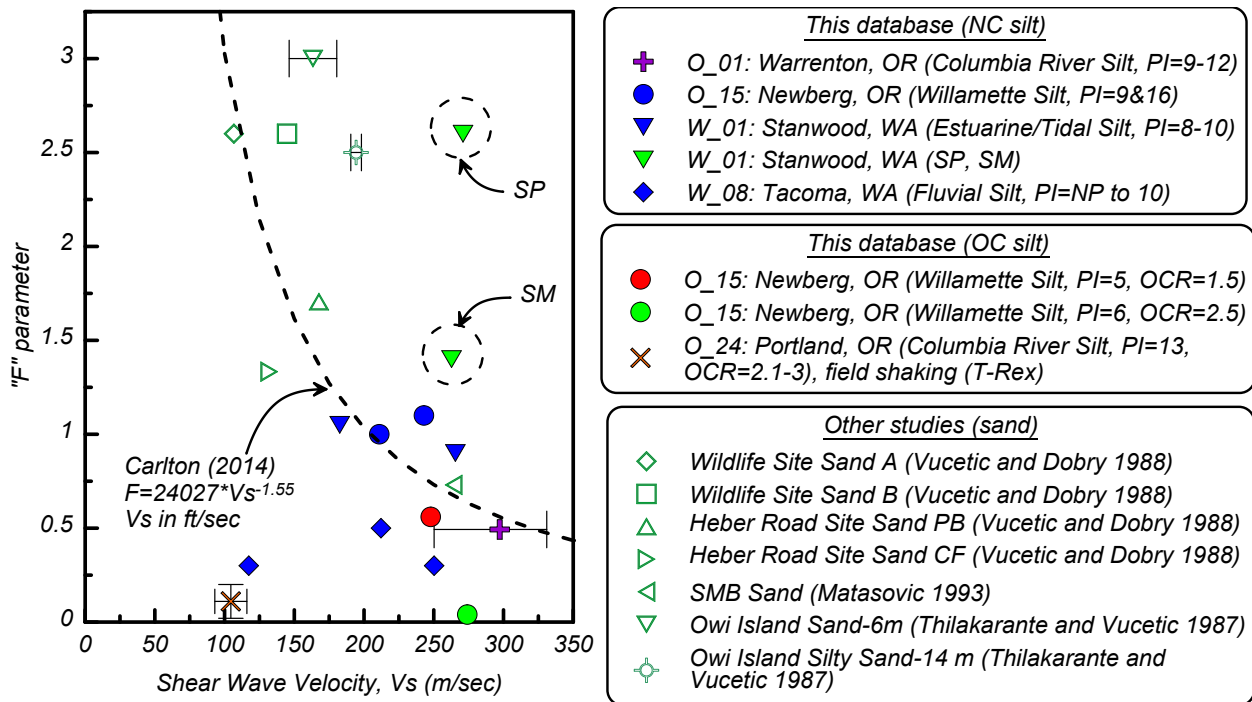


Figure 11: Variation between Parameter F in the Vucetic and Dobry model and the shear wave velocity (V_s).

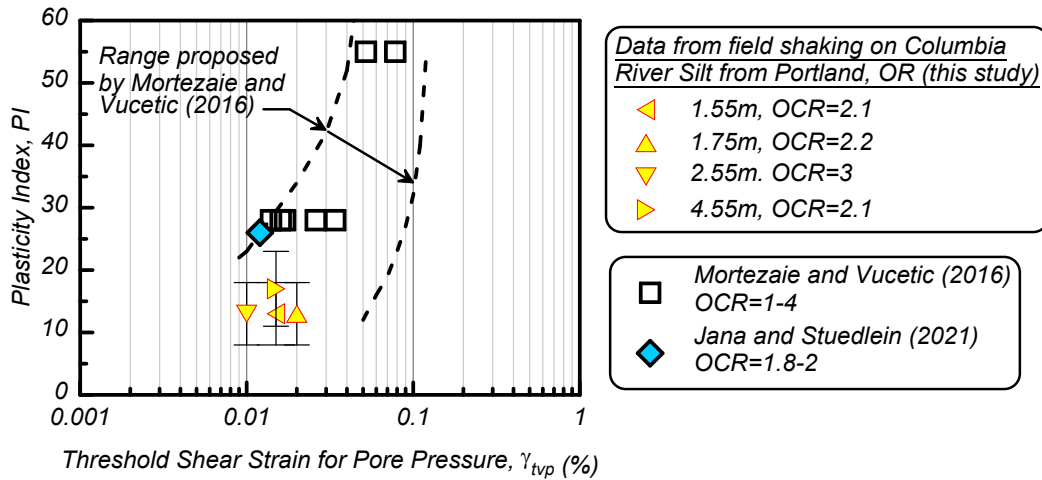


Figure 12. Comparison of threshold shear strain for cyclic pore water pressure generation (γ_{tp}) from this study and the data reported by Mortezaie and Vucetic (2016) and Jana and Stuedlein (2021).

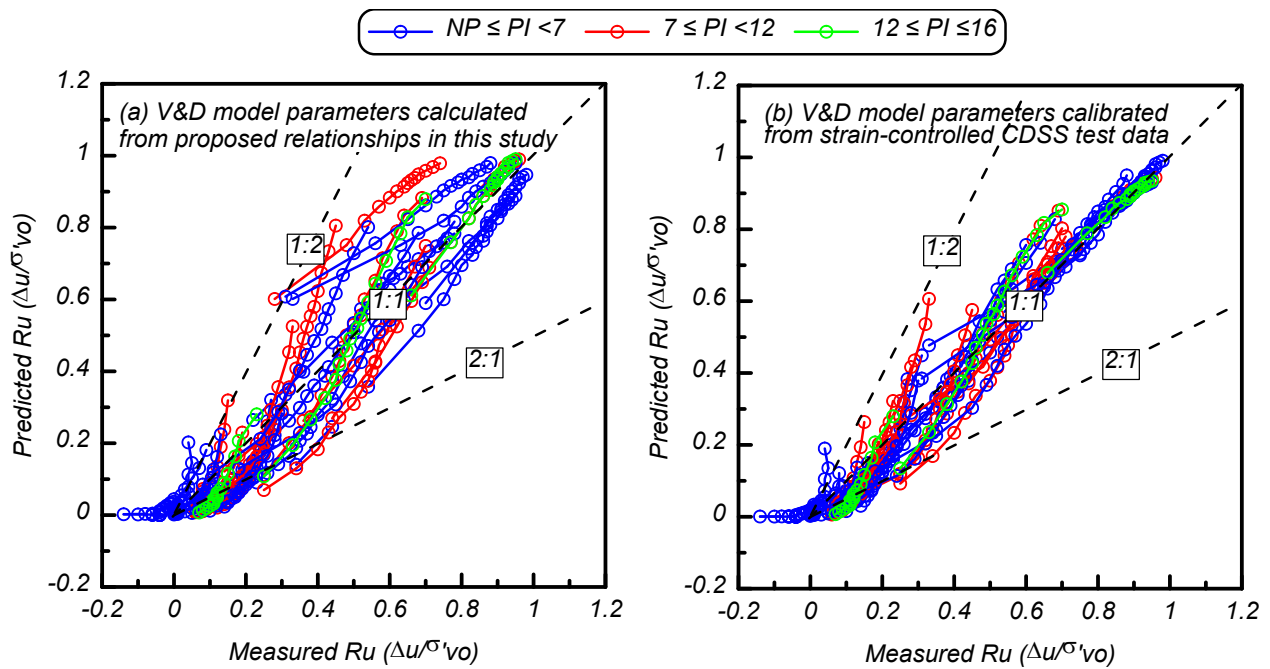


Figure 13: Comparison between measured and predicted pore pressure ratios for (a) V&D model parameters calculated using the proposed predictive equations in this study and (b) V&D model parameters calibrated based on the test data.